

Electronic Thesis and Dissertation Repository

8-9-2021 10:00 AM

The Role of Circular RNA HIPK3 in Ischemia Reperfusion Injury During Heart Transplantation

Adam P. Greasley, *The University of Western Ontario*

Supervisor: Dr. Xiufen Zheng, *The University of Western Ontario*

Co-Supervisor: Dr. Dave Nagpal, *London Heath Sciences Centre*

A thesis submitted in partial fulfillment of the requirements for the Master of Science degree in Pathology and Laboratory Medicine

© Adam P. Greasley 2021

Follow this and additional works at: <https://ir.lib.uwo.ca/etd>

Recommended Citation

Greasley, Adam P., "The Role of Circular RNA HIPK3 in Ischemia Reperfusion Injury During Heart Transplantation" (2021). *Electronic Thesis and Dissertation Repository*. 8046.
<https://ir.lib.uwo.ca/etd/8046>

This Dissertation/Thesis is brought to you for free and open access by Scholarship@Western. It has been accepted for inclusion in Electronic Thesis and Dissertation Repository by an authorized administrator of Scholarship@Western. For more information, please contact wlsadmin@uwo.ca.

Abstract

There are currently ~600,000 Canadians with end stage heart failure. Although medications are effective, the ideal treatment would be heart transplantation. Loss of blood (ischemia) to the organ during preservation and restoration of blood flow (reperfusion) leads to ischemia reperfusion injury (IRI) which can lead to cell death. Circular RNA is a new type of non-coding RNA forming a covalently closed loop single stranded RNA. Evidence suggests circular RNA Hipk3 (circHIPK3) generated from exon 2 of the Hipk3 gene is involved in many pathologies. However, the role of circHIPK3 in IRI has not been investigated. Using our *in vitro* IRI model, we showed that CircHIPK3 expression is increased during IRI and knockdown increased cell death. In addition, circHIPK3 knockdown exacerbated pro-apoptotic Bax mRNA levels, caspase 3 activation and MLKL phosphorylation. We also observed no significant changes in inflammatory response following circHIPK3 knockdown and IRI. In conclusion, the loss of circHIPK3 expression exacerbates apoptosis and necroptosis during IRI and is crucial to cell survival.

Keywords: Circular RNA, CircHIPK3, Ischemia Reperfusion Injury, Heart Transplantation,

Lay Abstract

Heart diseases is a leading cause of death world-wide and the second leading cause of death in Canadians. Although we have developed many successful treatments for end-stage heart failure, the best treatment would be to replace the organ with a heart transplantation. However, loss of blood flow (ischemia) for long periods and restoring of blood (reperfusion) can leading to ischemia reperfusion injury (IRI) and cause the cells and the organ to die or exert extra damage in the recipient. IRI is a large barrier that prevents many hearts being viable from donors, with only 24% of donors having a viable heart. Therefore, the need to help the success rate of transplant surgeries and increase the availability of donors is immense. A new molecule known as circular RNA (circRNA) involvement in human disease is becoming increasingly important. CircRNA can act as a regulator by effecting other types of RNA or proteins involved in many diseases. Circular RNA Hipk3 (circHIPK3), has been identified as a key centre point in cell survival. However, circHIPK3s role in IRI has not been studied. Our research shows that circHIPK3 expression can directly influence the outcome of successful preservation. Our results showed that decreases in circHIPK3 leads to increased death during reperfusion and provides worse outcomes. This suggests that circHIPK3 plays a vital role in IRI and that its levels may be useful to determine the difference between successful and unsuccessful organ preservation. Success of this research will provide insight into previously unknown targets for IRI treatment and help develop new therapies. This in turn will allow us to increase the availability of heart donors and decrease the number of patients on the waiting list.

Acknowledgements

I would like to acknowledge the immense guidance and support of my supervisors Dr. Xiufen Zheng and Dave Nagpal who have been nothing but supportive and guiding throughout my masters experience. Dr. Zheng in particular helped me approach experimental problems in new ways improving my ability to come up with experimental ideas, tests my hypotheses and draw inclusion. She has done this repeatedly for two years while always supporting my more creative ideas and providing g a pleasant and enriching learning environment. Dr. Zheng was also responsible for assisting me with the design, conduction and data analysis of this thesis. I would also like to acknowledge my lab manager Dr, Xizhong Zhang and my lab mates Bowen Wang, Shuailong Li and Qinfeng Zhou who were always very supportive and made the lab a fun place to be. I would also like to extend my deepest gratitude to my advisory committee members Dr. Weiping Min and Dr. Alp Sener, both of whom have been supportive and provided important guidance throughout my project.

Table of Contents

Abstract.....	II
Lay Abstract.....	III
Acknowledgements.....	IV
List of Tables.....	VII
List of Figures.....	IX

Contents

Chapter 1. Introduction to Ischemia Reperfusion Injury and Circular RNA	1
1.1 Heart Disease and the Need for Heart Transplantation	1
1.2 Heart Transplantation Availability and the Ischemia Reperfusion Barrier	3
1.3 Ischemia Reperfusion Injury and Reactive Oxygen Species Generation	4
1.4 Ischemia Reperfusion Injury Induced Cell Death.....	6
1.4.1 Intrinsic and Extrinsic Apoptosis.....	7
1.4.2 Caspase Independent Form of Cell Death	8
1.5 Current Treatment and Protective Strategies for Ischemia Reperfusion Injury	9
1.6 Circular RNA: a new type of non-coding RNA.....	11
1.7 Circular RNA Hipk3: A Highly Abundant and Distributed Circular RNA.....	13
1.8 CircHIPK3 in Disease.....	14
1.8.1 CircHIPK3 in Diabetes	15
1.8.2 CircHIPK3 in Cancer.....	16

1.8.3 CircHIPK3 and Fibroblast Differentiation.....	17
1.8.4 CircHIPK3 in Ischemia Reperfusion Injury	17
1.9 Hypothesis Statement.....	20
Chapter 2. Materials and Methods	21
2.1 Cell Culture.....	21
2.2 Primary Cardiomyocyte Culture (PCM).....	21
2.3 Ischemia and Reperfusion Injury Model.....	22
2.4 CircHIPK3 siRNA mediated knockdown.....	23
2.5 Real-time Cell Death using an Incucyte System.....	24
2.6 Cell Apoptosis and Death Quantification by Flow Cytometry.....	24
2.7 RNA Isolation	25
2.8 cDNA generation	25
2.9 Quantitative Polymerase Chain Reaction (qPCR)	26
2.10 CircHIPK3 primer validation.....	28
2.11 Lactate Dehydrogenase (LDH) Assay	29
2.12 Protein Isolation and Western Blotting.....	29
2.13 Statistical Analysis.....	31
Chapter 3. Results	32
3.1 CircHIPK3 expression increases during cardiac IRI	32
3.2 CircHIPK3 knockdown prior to IRI leads to increased cell death.....	35

3.3 CircHIPK3 knockdown leaves cells vulnerable to IRI	38
3.4 CircHIPK3 knockdown exacerbates apoptosis and necroptosis during IRI	40
Chapter 4. Discussion	45
4.1 CircHIPK3 expression increases in myocardial IRI	45
4.2 CircHIPK3 knockdown leads to increased cell death during IRI	46
4.3 CircHIPK3 as a suppressor of apoptosis.....	47
4.4 CircHIPK3 knockdown promotes apoptosis through intrinsic signalling	48
4.5 CircHIPK3 knockdown leads to increased necroptosis	50
4.6 Clinical Implications and Future.....	50
4.7 Conclusion and Future directions	51
Chapter 5. References	53

List of Tables

Table 1.1 Percentage of each organ used for donation from a donor.....	4
Table 2.1 1x D-Hanks recipe prepared for PCM isolation from neonatal C57/B6 mice.....	22
Table 2.2 Detailed information and transfection reagent amounts for siRNA mediated knockdown in HL-1 cardiomyocytes.....	24
Table 2.3 All primers used for qPCR and their sequences from 5' – 3' orientation.....	28
Table 2.4 Table of all primary antibodies used and their respective dilution.....	31

List of Figures

Figure 1.1 Number of cardiac related deaths per year in Canada showing increasing trend over time.....	1
Figure 1.2 Typical progression of heart disease from at risk conditions to congestive heart failure.....	2
Figure 1.3 Graphical summary of intrinsic and extrinsic apoptotic signalling and their interaction with necroptosis.....	9
Figure 1.4 Simplified example of back-splicing to produce exon-exon joining compared to exon circularization.....	13
Figure 1.5 Summary of different diseases and pathologies circHIPK3 has been investigate in and the respective miRNA studied.....	19
Figure 2.1 Divergent primers and their use to amplify circRNA across their back-splice junction distinguishing them from their linear counterpart and traditional primer design.....	27
Figure 3.1 Expression of circHIPK3 is increased during IRI.....	34
Figure 3.2 CircHIPK3 knockdown prior to IRI increases cell death and damage.....	37
Figure 3.3 CircHIPK3 knockdown leaves cell vulnerable to apoptosis.....	39
Figure 3.4 CircHIPK3 knockdown exacerbates cell death through activation of apoptosis during IRI.	42
Figure 3.5 CircHIPK3 knockdown exacerbates necroptosis during IRI.....	44

Chapter 1. Introduction to Ischemia Reperfusion Injury and Circular RNA

1.1 Heart Disease and the Need for Heart Transplantation

Heart disease remains the second leading cause of death in Canada, killing 51,000-53,000 Canadians per year between 2015-2019¹. The death toll from heart disease is on the rise, where 48,757 cardiac related deaths occurred in 2010 compared to the 52,541 in 2019 (Figure 1.1).

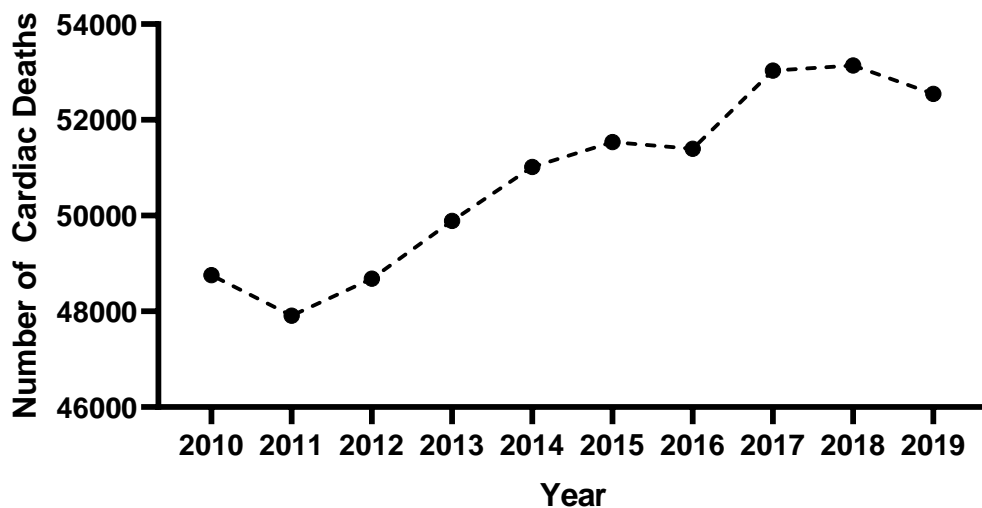


Figure 1.1: Number of cardiac related deaths per year in Canada showing increasing trend over time. Data obtained from stats Canada¹.

In 2013 it was estimated that 2.4 million Canadians were living with diagnosed heart disease (HD) a steep rise from the 1.5 million in 2001. Although the prevalence of HD in Canadians and absolute deaths has risen, the percentage of deaths has dropped with an increase in survival of acute HD due to effective treatments and increased awareness of

signs and symptoms. As survival rates of acute myocardial injuries and conditions increases, the number of patients who develop end stage heart failure or congestive heart failure increases. Patients who survive acute HD are six times more likely to develop structural changes in the heart and symptoms associated with end stage heart failure, in which the heart lacks the ability to pump blood and supply the other organs and body with the oxygen and nutrients required (Figure 1.2).

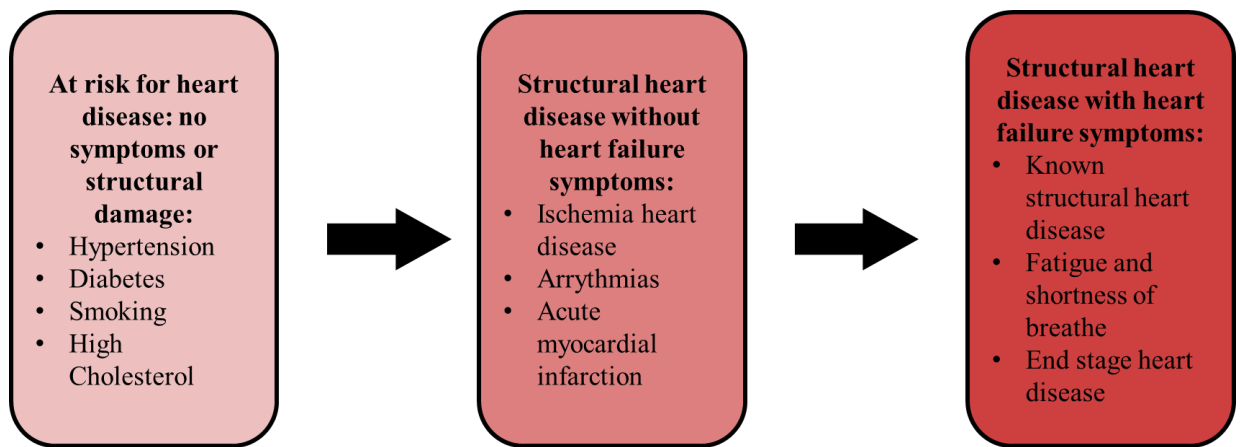


Figure 1.2 Typical progression of heart disease from at risk conditions to congestive heart failure.

It is estimated that there are currently 600,000 Canadians living with heart failure, with an increasing incidence there is an increased demand for transplantation.² Although most cases can be managed by lifestyle, medications or minor surgical procedures, when these treatments fail patients may be candidates for heart transplantation. In 2011, the Canadian Cardiac Transplant Network published a report for eligibility of recipients in Canada. They cited any late stage heart failure as criteria for recipients to be eligible, given there are no pre-existing conditions that would cause heart failure immediately or poor surgical outcomes.³ However, they summarized that the largest limiting factor being low numbers

of eligible donors. In 2019, there were a total of 346 patients placed on the waiting list, 189 of which received heart transplantation.⁴ This translates to 54.6% of patients receiving a transplant however, their length of time on the waitlist is not listed, which could span months to years. In the coming years as the prevalence of end stage heart failure increases, the need for heart transplantation and eligible donors will increase.

1.2 Heart Transplantation Availability and the Ischemia Reperfusion Barrier

Ischemia reperfusion injury (IRI) characterized by loss of blood (ischemia) and full restoration of blood flow (reperfusion) can lead to cell death and tissue damage and remains a large barrier of eligible donors for heart transplantation. Due to this barrier, the availability of viable hearts from organ donors is largely diminished. In 2018, of the 189 heart transplantations performed in Canada, only 24% of donors were classified as previously deceased while 0% of donors were classified as donor after circulatory death (DCD) (Table 1.1).⁴ In contrast, in 2018 there was 1706 kidneys transplanted throughout Canada, 86% of these transplantations were from previously deceased donors compared to the 24% of cardiac transplants. In addition, 30% of donors were classified as DCD, which represents approximately 29% of all deceased donors (Table 1.1). The inability to use a large percentage of deceased donors and DCD largely limits the availability of hearts. DCD and deceased donors are not considered eligible due to the increased IRI and risk of worse outcomes. During ideal organ preservation, the donor body is cooled and the steps to preserve the organ are taken prior to ischemia occurring, where as in DCD the ischemia period begins prior to preservation leading to periods of warm ischemia which can be detrimental to organ viability after reperfusion.⁵ There is a clear relationship between longer lengths of ischemia leading to greater chance of post-operative ventricular

failure^{6,7}, along with revascularization and direct myocardial infarction.^{8,9} Therefore, to increase the availability of donor hearts, it needs an effective strategy to mitigate IRI and improve organ preservation in cardiac transplantation.

Table 1.1 Percentage of each organ used for donation from a donor.

Organ type	Proportion of deceased donors having an organ used for transplantation	Proportion of organs from DCD
Kidney	86% at least one kidney 79% both kidneys	30%
Liver	60%	10%
Heart	24%	0%
Lung	42% at least one lung 38% both lungs	27%
Pancreas	9%	10%

1.3 Ischemia Reperfusion Injury and Reactive Oxygen Species Generation

Ischemia reperfusion injury, where periods of ischemia lead to organ death yet full reperfusion leads to further tissue injury, remains an important paradox and concept that challenges organ transplant for the past 50 years⁸. It is well known that ischemia leads to organ dysfunction through depletion of cellular ATP due to lack of mitochondrial function in which tissues becomes necrotic and undergo irreversible cell death^{5,8,10-12}. Therefore, guidelines and procedures have been developed to assist in minimizing ischemia times and predict which organs are viable. The standard of care for cardiac transplantation currently revolves around the concept of preventing ischemia before organ preservation begins and mitigating ischemic times by restoring blood flow quickly^{5,6,12-14}. Although procedures and preservation methods such as cardioplegia solutions such as university of Wisconsin (UW)^{15,16} solution have greatly reduced the effects of ischemia⁸,

the time between donor harvest and transplantation in a recipient takes several hours. This means ischemia is not fully mitigated and although necrosis rarely occurs, the effects of reperfusion injury are always present. Reperfusion injury is driven primarily by the acute increased generation of reactive oxygen species (ROS) and reactive nitrogen species (RNS) after reintroduction of oxygen as mitochondria begin to produce ATP again^{8,10,17}. This sudden and increased generation of ROS/RNS out paces the cellular ability to detoxify these substances, creating an imbalanced redox signalling pathway.^{8,18} Part of this imbalance is generated in early ischemia, where cellular metabolism shifts from oxidative phosphorylation and Beta-oxidation to make ATP through anaerobic methods such as glycolysis at the expense of reductive molecules, leaving the NADH/NAD⁺ ratio to increase and the cellular ability to remove free radicals impaired¹⁹. Under normal conditions, ROS such as $O_2^{\bullet-}$ are generated in low amounts through electron leakage of the inner mitochondrial membranes during oxidative phosphorylation²⁰⁻²². Any free radicals that are generated quickly undergo single electron reduction to generate stable molecules. The exact mechanism depends on their location within the mitochondria, while both the matrix and intermembrane space both contain superoxide dismutase, the intermembrane space contains cytochrome C and the Q_0 site of complex III, while the Q_i site of complex III is orientated towards the matrix^{20,23,24}. During ischemia, there is a modest increase in free radicals, but more importantly there is an impairment of cytochrome oxidase dimer formation and a depletion of cytochrome C²⁵, impairing the scavenging of ROS in the mitochondrial matrix and intermembrane space. In addition, superoxide dismutase interacts with $O_2^{\bullet-}$ and yields larger proportions of H_2O_2 , which accumulate in the cell and activate RNS^{8,21,22}. Although there is a shift in generation of ROS during ischemia, this pathway is self-limiting as the primary $O_2^{\bullet-}$ depends on the

presence of O₂, in which there is none and the ROS levels do not near fatal limits^{26,27}.

High levels of ROS are only achieved during reperfusion phase in which oxygen is reintroduced to mitochondria and O₂^{•-} can once again be generated, but at greater quantity than prior to ischemia. Once ROS during reperfusion reach a high enough threshold, they induce cellular damage and death through activation of proteolytic enzymes, metalloproteases, membrane damage and further mitochondrial dysfunction²⁸. Therefore, it is the shift of available O₂ to ROS and the inhibition of ROS detoxification during ischemia and the restoration of O₂ and ROS generation during reperfusion that drive IRI and fatal limits of ROS.

1.4 Ischemia Reperfusion Injury Induced Cell Death

Prolonged ischemia reperfusion injury is capable of inducing significant cellular stress and eventual death. Typically, there are four modes of cell death during IRI. Necrosis and necroptosis share a pro-inflammatory form of cell death, while apoptosis and mitoptosis share more regulated and controlled form of cell death¹¹. Necroptosis and necrosis share similar characteristics such as cellular swelling, membrane permeability and lack of chromatin. Where apoptosis and mitoptosis are controlled forms of cell death resulting in shrinkage of cellular bodies, pyknosis of the nucleus and controlled degradation of cellular components²⁹. Mitoptosis refers directly to death of mitochondria leading to apoptosis and/or autophagy: controlled degradation of the own cell. While apoptosis can occur both in a mitoptosis dependent or independent manner, apoptosis is energy-dependent and requires a series of molecular checkpoints driven by proteolytic cleavage and enzyme activation^{18,29,30}. There are three characterized apoptotic pathways, the extrinsic regulated through death factors and ligand binding, the intrinsic largely

regarded as the mitochondrial activation pathway, and granzyme pathway which is regulated through T-cell activation²⁹. Due to the similarities between necroptosis and necrosis, along with mitoptosis' dependency on apoptosis, we have chosen to focus on necroptosis and apoptosis throughout this thesis.

1.4.1 Intrinsic and Extrinsic Apoptosis

During IRI, the extrinsic and intrinsic pathways both show activation and have an interplay previously thought to be mutually exclusive²⁹⁻³¹. During reperfusion as ROS reach fatal levels and the pH rises within the mitochondria the mitochondria permeability transition pore (mPTP) begins to open^{18,32}. mPTP activation can occur through membrane integrity loss due to ROS damage causing Ca²⁺ overload^{31,33} or activation of B-cell lymphoma 2 (Bcl-2) protein family^{18,31,32,34}. Bcl-2 family of pro-apoptotic proteins initiates mPTP through the oligomerization of Bcl-2 associated X protein (Bax) and Bcl-2 homologous antagonist killer (Bak), allowing cytochrome C and ROS release from mitochondrial matrix to the cytosol³³. Other Bcl-2 family proteins such as B-cell lymphoma-extra large (Bcl-XL) play an anti-apoptotic role aimed at preventing cytochrome C release and can be targeted to prevent or exacerbate intrinsic apoptosis. The terminal end of the intrinsic apoptotic signalling pathway is marked by cytochrome C release and procaspase 9 aggregation and subsequent activation to caspase 9. The extrinsic pathway of apoptosis is mediated through binding of ligands to death receptors and caspase activation. The most well defined of these are the TNF α /TNF receptor 1 and Fas Ligand/Fas Receptor. In the extrinsic model, activation of receptor proteins results in TRADD and/or FADD recruitment and association with procaspase 8 forming the death inducing signalling complex (DISC)^{29,35}. DISC leads to caspase 8 cleavage and

subsequent activation at the terminal end of the extrinsic signalling pathway^{29,31}.

Regardless of intrinsic or extrinsic activation, both apoptotic signalling pathways end with the activation of effector caspases such as caspase 3. Effector caspase activation marks the beginning of the execution pathway, in which endonucleases, proteases, and degradation of cellular component begin along with morphological change^{29,31,36}.

1.4.2 Caspase Independent Form of Cell Death

An alternative form of cellular death induced by IRI is necroptosis. Necroptosis is a programmed cell death that is independent of caspase activation and appears to be exclusive with extrinsic apoptotic signalling. During necroptosis, TNF α induced FADD activation recruits receptor-interaction serine/threonine kinase 1 (RIP1) and receptor-interaction serine/threonine kinase 3 (RIP3) cross-phosphorylation and their complex formation of the necrosome³⁷⁻³⁹. The necrosome then leads to phosphorylation of mixed lineage kinase domain like protein (MLKL)³⁷. P-MLKL along-side necrosome formation is responsible and essential for necroptosis and cell death that is mechanistically and physiologically distinct from apoptosis. Both RIP1 and RIP3 are known targets of caspase 8 cleavage^{40,41}, suggesting that activation of extrinsic apoptosis is mutually exclusive, or at least not inducing of necroptosis, while intrinsic apoptosis can co-exist in theory. A summary of apoptotic and necroptosis signalling can be found in Figure 1.3.

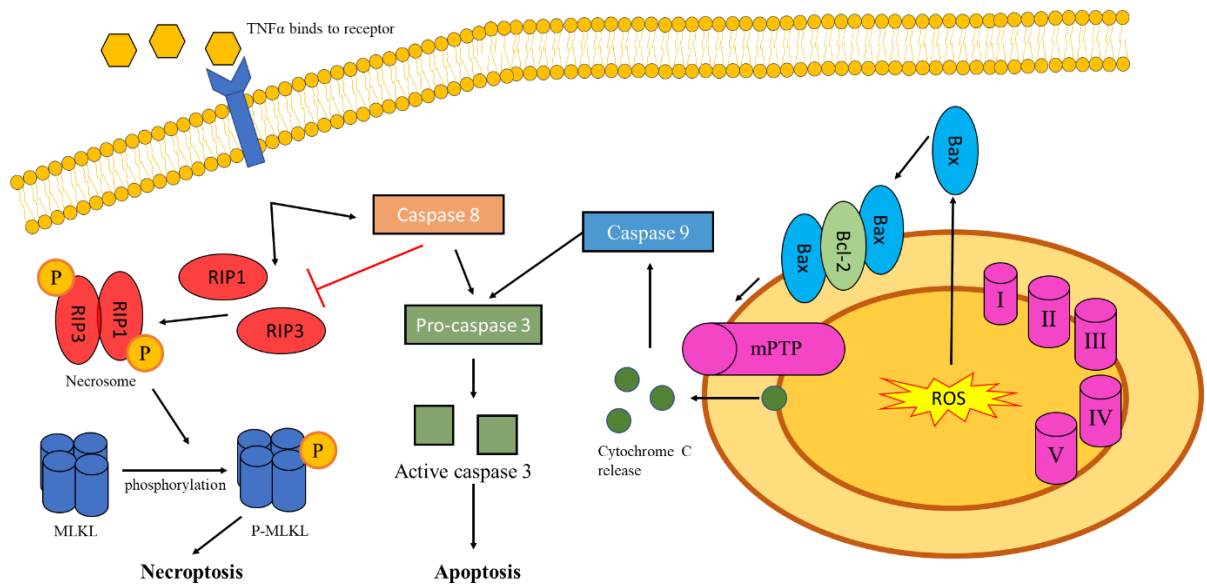


Figure 1.3 Graphical summary of intrinsic (right) and extrinsic (centre) apoptotic signalling and their interaction with necroptosis (left).

1.5 Current Treatment and Protective Strategies for Ischemia Reperfusion Injury

IRI remains a leading complication during cardiac transplantation and although research progress in the past 40 years has been successful in mitigating IRI to some extent, no standard of care or drugs have been accepted world-wide. The initial treatment for IRI is recognized as ischemic pre-conditioning in which small episode of ischemia is used to produce a cardio protective effect prior to an induction of a long ischemic episode. This was first observed in 1986 where smaller infarct size was observed following long term ischemia in samples which had smaller intervals prior⁴². There is evidence suggesting changes in metabolic state which provide protective effects for up to 72 h following pre-conditioning⁴³⁻⁴⁵. Although mechanistically pre-conditioning is complex and not well understood, there are theories supporting it dampens the burst of ROS during reperfusion phase as well as increasing pro-survival signals such as ERK1/2 during the short term ischemia through ROS generation⁴⁶. The activation of ATP-

sensitive Potassium (K_{ATP}) channels during pre-conditioning is thought to be important for mitochondrial stability and reduce Ca^{2+} over-loading and influx during ischemic insult, lowering MPTP formation and leading to protection against long term hypoxia^{46,47}. Although pre-conditioning is a promising treatment that has been shown experimentally and clinically, it can only be applied in situations where long-term ischemia can be anticipated such as cardiac by-pass surgery. This makes it more complicated to involve during organ transplantation where anticipation is not always possible especially with previously deceased patients. Therefore, alternative treatments have been a focus of research for the past 30 years.

Preventing mPTP formation through ROS scavenging is a thoroughly researched concept in cardiac surgery⁸. Increasing endogenous levels of natural antioxidants has been tried and shown potential, but sometimes it can be deleterious due to the absence of any redox signalling of pro-survival signals prior to ischemia. Therefore, emphasis on external drugs such as N-acetylcysteine, ebselen, allopurinol and α -tocopherol has been tested^{8,18,48,49}. Experimental evidence suggests these are effective at scavenging and reducing ROS during IRI, but due to the low efficacy of delivery to the mitochondria *in situ*, their clinical applicability limited. Other compounds designed with mitochondrial targeting abilities such as mitoquinone have been shown to be effective when delivered prior to IRI^{18,50}. More recently, AP39, a hydrogen sulfide releasing agent has shown efficacy at protecting against IRI in kidney⁵¹, although its effect on cardiac IRI remain primitively studied⁵².

It is clear in the past 50 years much progress at understanding and protecting against IRI has been made through surgical strategies and drugs. However, there is no

clear solution or standard that can completely mitigate IRI as many treatments are situationally dependent or require specific routes of administration that may be unfeasible. Therefore, new treatments and regulators of IRI are needed.

1.6 Circular RNA: a new type of non-coding RNA

Circular RNA (CircRNA) are a novel non-coding RNA that have become an increasing topic of interest involved in the pathogenesis of diseases^{53,54}. CircRNA was first observed in 1976 under electron microscopy and recognized as nothing more than mis-splicing and splicing errors⁵⁵. However, recent advances in molecular biology techniques and bioinformatics pipelines have led to their re-discovery as important, and possible the largest family, of non-coding RNAs with an estimate of >20,000 unique human CircRNAs^{56,57}. Although the estimated amount of CircRNA remains theoretically possible, it is likely a smaller subset of them are transcribed *in vivo* at biologically relevant levels. CircRNAs are a single stranded covalently closed loops of RNA, characterized by their lack of polarity, poly-A tail and stability *in vivo*^{58,59}. CircRNA are generated through a process known as back-splicing of the pre-mRNA using the canonical splicing machinery and competes with mRNA biogenesis⁵⁸. In canonical splicing, a conserved GU element at the 5' end of the intron and an AG at the 3' end; termed the donor and acceptor site respectively are crucial for exon joining^{53,60}. The protein-mRNA complex known as the spliceosome, catalyzes the nucleophilic attack of a 2' OH of an adenosine molecule 20-50 nucleotides upstream of the acceptor site known as the branching point onto the 5' phosphate of the donor site⁶¹. This attack forms a covalent loop known as the lariat. The newly free 3' OH of the upstream exon attacks the 5' phosphate of the acceptor site, joining the exons and releasing the lariat introns. During

back-splicing, CircRNA have been proposed to be formed through two mechanisms: direct backs-splicing or exon skipping^{58,61}. In exon skipping of a 3-exon pre-mRNA, the branching point of intron 2 would attack the donor site of intron 1, followed by the attack of the 3'OH from exon 1 onto the acceptor site of intron 2^{53,58}. This would result in the joining of exons 1 and 3, with the release of introns 1, 2 and exon 2 as the lariat. The resulting circRNA may contain exon/intron sequences or undergo further nucleophilic attack to allow the release of exon 2 as CircRNA, and an intronic lariat by-product^{53,59}. In direct back-splicing of a similar pre-mRNA, the pre-mRNA molecule will form a secondary structure between introns 1 and 2. The branching point of intron 1 will attack the donor site of intron 2, resulting in a 3'OH on exon 2. The 3'OH attacks the acceptor site on intron 1, releasing exon 2 as a CircRNA, and a terminated fork product⁵⁹. A simplified concept of back-splicing can be seen in Figure 1.4.

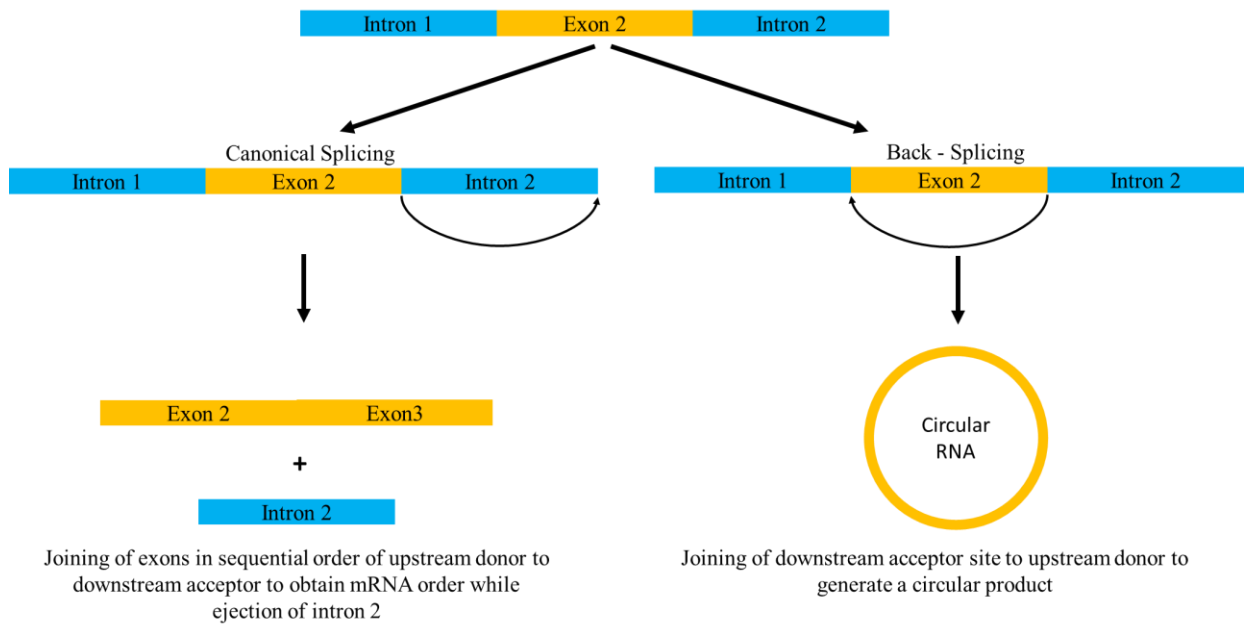


Figure 1.4 Simplified example of back-splicing to produce exon-exon joining compared to exon circularization.

1.7 Circular RNA Hipk3: A Highly Abundant and Distributed Circular RNA

Recently, a circular RNA derived from exon 2 of homeodomain-interacting protein kinase 3 (Hipk3), termed circular RNA Hipk3 (circHIPK3), has become an increasing target of interest for therapeutic research. The biogenesis of circHIPK3 has been partially eluted. Recent studies suggest the secondary structure of the pre-mRNA-spliceosome complex is mediated through short intronic repeat sequences (SIRS) in the flanking introns^{56,62}. Zheng et al showed SIRS to be crucial for circHIPK3 biogenesis⁵⁶. Flanking intron analysis of exon 2 of HIPK3 showed complementary 28 SIRS upstream and 51 SIRS downstream of circHIPK3. Two SIRS elements immediately flank exon 2 of HIPK3 upstream and downstream. Subsequent deletion suggests that the downstream SIRS are crucial for circHIPK3 biogenesis⁵⁶. Interestingly, upstream SIRS mutations had no effect on circHIPK3 biogenesis, likely due to further upstream SIRS which can

facilitate a similar circularization reaction, which was confirmed by CRISPR/Cas9 knockout of intronic repeats⁵⁶. The mutations of intronic sequences reportedly had no effect on HIPK3 mRNA production, but showed significant downregulation of circHIPK3, indicating that SIRS elements are crucial for circHIPK3 biogenesis. Other circRNA variants of the HIPK3 gene have been detected however, their relative abundance is low when compared with circHIPK3 derived solely of exon 2⁵⁶. More recently, RNA binding protein quaking (QKI) has been shown to play an important role in circRNA biogenesis, by binding to QKI response elements in the flanking introns^{63,64}. Addition or deletion of QKI response elements is sufficient to promote/diminish but not abolish circRNA biogenesis⁶³. Therefore, it is likely both SIRS elements and RNA binding proteins are essential for circRNA biogenesis. However, the presence of QKI response elements and QKI function on circHIPK3 has yet to be investigated.

1.8 CircHIPK3 in Disease

CircRNA function, regulation and mechanisms remain largely unstudied in cells however, there is increasing evidence of their abilities to act as RNA-binding protein and micro RNA (miRNA) sponges^{65,66}. miRNAs are 19-25 nucleotide non-coding RNA's which bind to the 3' untranslated region (3' UTR) of mRNA molecules⁶⁷. miRNA act as a guide to the RNA-induced silencing complex (RISC), which leads to subsequent 3'-to-5' mRNA degradation through Ago2^{65,67}. The polarity of linear mRNA is essential for endonuclease degradation. The lack of polarity of circRNA molecules renders circRNA inert to Ago2 cleavage when bound with miRNA^{65,68}. CircRNA resistance to endonuclease likely contributes to their long half-life, > 24 h, and high stability *in vivo*. Recently, circHIPK3 has been implicated to have tumorigenesis⁶⁹⁻⁷¹ and metabolic^{72,73}

regulatory properties, acting primarily as an miRNA sponge. Through luciferase reporter assays and miRNA library screening, circHIPK3 has been proposed to interact with ~10 miRNA across a variety of diseases and cell types. circHIPK3 has been studied in a variety of diseases, including diabetes, fibroblast differentiation, cancer and cardiac disease.

1.8.1 CircHIPK3 in Diabetes

High-glucose has been proposed to regulate circHIPK3 expression both *in vitro* and *in vivo*⁷²⁻⁷⁴. circHIPK3 levels were increased in retinal endothelial cells of diabetic mice in a time dependent manner⁷². Further bioinformatics analysis lead to the determination that high glucose and oxidative stress can increase circHIPK3 expression through c-myc transcription factor⁷². Chromatin immunoprecipitation showed increase c-myc binding to the promoter of HIPK3 gene during oxidative stress and high glucose conditions⁷². In addition, c-myc silencing normalized circHIPK3 expression levels in high glucose mice. HIPK3 mRNA levels were not reported however, it could prove crucial to understand where circHIPK3 level under high glucose/oxidative stress is regulated at the parent gene, spliceosome or both. *In vitro*, overexpression of circHIPK3 increased the viability, migration and proliferation of human retinal vascular endothelial cells (HRVECs)⁷². CircHIPK3 mechanism was proposed to act primarily through sponging miR-30 and affecting angiogenic factors such as endothelial growth factor-C (VEGFC), FZD4 and WNT2 signalling⁷². VEGFC, FZD4 and WNT2 are targets of miR-30 and silencing/expression of circHIPK3 leads to angiogenic factor suppression/expression respectively. A second study using human serum showed a similar increase in circHIPK3 in type 2 diabetic patients and a positive correlation

between circHIPK3 levels and neuropathic pain⁷⁴. A diabetic rat model showed circHIPK3 to regulate inflammatory signalling through sponging miR-124⁷⁴. In contrast, a recent study showed high-glucose in human umbilical vein endothelial cells (HUVECs) and diabetic patients experience decreased levels of circHIPK3⁷³. Primary human aorta endothelial cells showed similar downregulation of circHIPK3 induced by high-glucose diet environment⁷³. Cao et al, 2018 propose that lower levels of circHIPK3 leads to increased miR-124 silencing leading to apoptosis and cell death⁷³. Between both studies, it is clear that circHIPK3 functions as an miR-124 sponge to influence inflammatory signalling, however circHIPK3's role as a potential diagnostic marker remains unclear.

1.8.2 CircHIPK3 in Cancer

To date, the most widely studied implication of circHIPK3 metabolism is its involvement in cancerous cell types and tissues, including prostate^{75,76} and bladder^{77,78}.

In prostate cancer, circHIPK3 was up regulated in prostate epithelial cells compared with normal tissue in humans⁷⁵. circHIPK3 was shown to target miR-338-3p, altering extracellular matrix remodelling similar as in fibroblast differentiation. Based on miR-338-3p expression, circHIPK3 appears to be primarily upregulated in patients in stage III-IV, when compared with early stage patients⁷⁵. A second study on prostate cancer confirmed circHIPK3 over expression and elucidate the role of miR-193a-3p and MCL1 regulation playing a role in cell apoptosis and proliferation⁷⁶. A notable feature of circHIPK3 in cancer is its correlation with prognosis. circHIPK3 silencing attenuates tumor progression and size, thus circHIPK3 may be used as a predictor of progression and prognosis of cancers and treatment.

In bladder cancer, a similar trend with circHIPK3 was observed. CircHIPK3 predicts and correlates with early stage bladder cancer prognosis and progression independently of the linear transcript⁷⁸. However, one study provides evidence that circHIPK3 is downregulated in bladder cancer tissue and cell lines⁷⁷. Li et al, 2017 suggests that lower circHIPK3 expression leads to increased miR-558 expression, facilitating heparinase expression.

1.8.3 CircHIPK3 and Fibroblast Differentiation

In addition to high-glucose environments, circHIPK3 has been shown to play a role in regulating fibroblast differentiation and proliferation⁷⁹⁻⁸¹. In a lung fibrosis model, circHIPK3 is upregulated and plays a role regulating fibroblast to myofibroblast differentiation⁷⁹. The increase in circHIPK3 expression leads to decreased miR-388-3p silencing by acting as a miRNA sponge⁷⁹. miR-388-3p targets mRNA of SOX4; a key regulator of mesenchymal modelling, and COL1A1; a main component of the extracellular matrix⁷⁹. Both SOX4 and COL1A1 are regulated through TGF- β signaling and are corner stones of fibrosis. Adversely, circHIPK3 silencing and miR-338-3p overexpression markedly protect and reverse fibroblast differentiation both *in vitro* and *vivo*⁷⁹. A similar study on cardiac fibrosis using an angiotension-II *in vitro/vivo* model shows parallel results; circHIPK3 is up-regulated in a fibrotic state and silencing of circHIPK3 attenuated fibrosis⁸⁰. This evidence provides insight into circHIPK3 as a potential target of therapies for pulmonary and cardiac fibrosis.

1.8.4 CircHIPK3 in Ischemia Reperfusion Injury

Recently, two studies have been published investigating the role of circHIPK3 in myocardial IRI. The first published by Bai et al. in 2019, showed that circHIPK3

expression was increased in human derived cardiomyocytes during short-term IRI⁸². Gain-of-function and loss-of-function studies showed that plasmid-based over-expression of circHIPK3 resulted in greater damage and increased cell death while siRNA attenuated injury. Bae et al. 2019 also showed that circHIPK3 increase exacerbated the expression of Bax and down-regulated Bcl-2, while sequestering the protective effects of miRNA-124-3p, aggravating IRI in cardiac cells. A similar study was performed by Qiu et al. in 2021, in which they showed circHIPK3 expression increase leads to exacerbated apoptosis and autophagy during cardiac IRI⁸³. The authors also showed increased Bax and reduced Bcl-2 in cells over-expressing circHIPK3 during IRI and increased cleaved caspase 3⁸³. In this study, Qui et al. showed evidence that circHIPK3 interacts with miRNA-20b-5p and the interaction is responsible for these effects observed⁸³. In contrast two studies showed the protective effects of circHIPK3 expression during myocardial IRI through activation of miR-29a/b pathway^{84,85}. Wang et al. 2019 showed that circHIPK3 expression was increased in hypoxia induced exosomes⁸⁶. Silencing of circHIPK3 lead to increased cell death and reversed the protective effects of hypoxia generated exosomes, while over-expressing in the exosomes resulting in increased cell viability and enhanced the protective effects⁸⁶. Wang et al. 2019 showed these effects were mainly contributed to the ability of circHIPK3 to sequester miR-29a and increasing IGF-1 expression⁸⁶. Similarly, Cheng at al. 2021 showed a protective effect in IRI using high glucose conditions to induce circHIPK3 expression and AKT3 signalling⁸⁵. circHIPK3 silencing lead to increased cellular apoptosis and an increase in proapoptotic genes through reduced sequestering of miR-29b, which was rescued by simultaneous over-expression of AKT3⁸⁵. The role of circHIPK3 in myocardial IRI remains controversial and requires

further investigation along with a standardized model to assess its cellular and molecular functions.

circHIPK3 has been implicated in many different mechanism and pathologies to date, most of which are quite recent. As the field of circRNA grows and new discoveries are made, the role of circHIPK3 in diseases will increase and its mechanisms made clear. A summary of the current development of circHIPK3 and its role in pathologies and miRNA targets can be found in Figure 1.5.

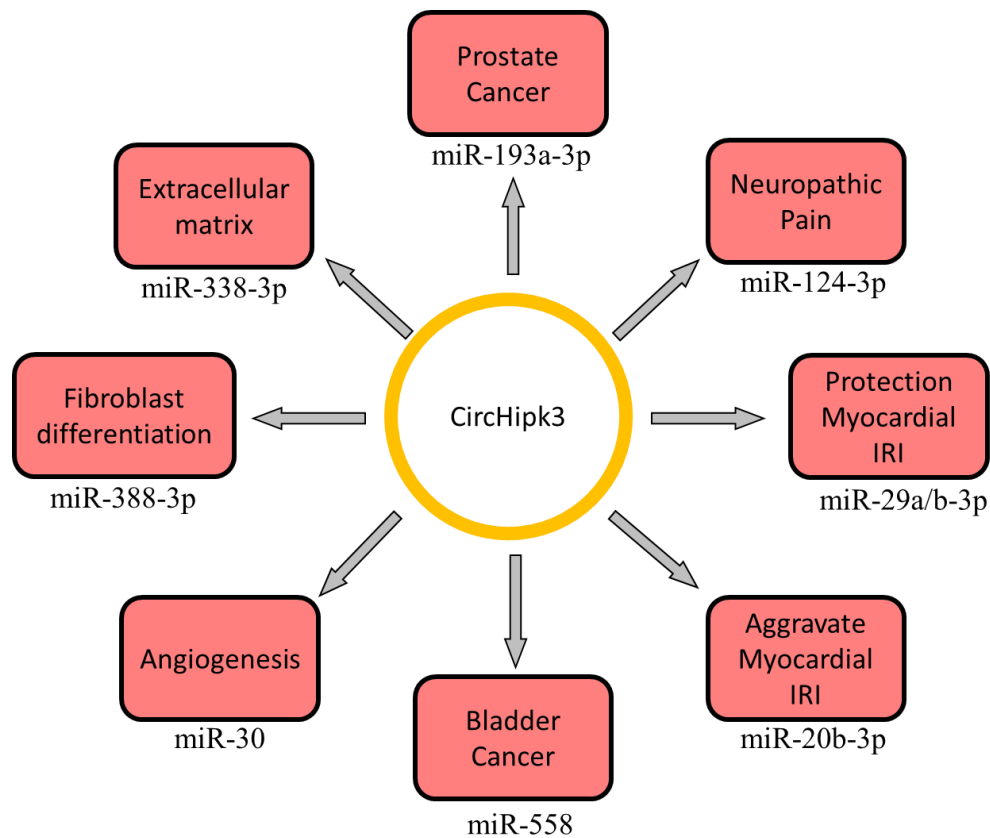


Figure 1.5 Summary of different diseases and pathologies that circHIPK3 has been investigate in and the respective miRNA studied.

1.9 Hypothesis Statement

Based on the role of circHIPK3 in many pathologies and its recent involvement in IRI, we believe circHIPK3 is a strong therapeutic target for cardiac IRI during heart transplantation. We **hypothesize** that circHIPK3 expression is increased during IRI following cold storage and that silencing of circHIPK3 will lead to exacerbated injuries. We aim to test the hypotheses through two aims. 1) Investigate the role of circHIPK3 expression on cell viability during IRI, 2) Investigate the underlying mechanism of circHIPK3 expression on cardiomyocyte viability during IRI.

Chapter 2. Materials and Methods

2.1 Cell Culture

Cardiomyocytes cell line HL-1 cells (Sigma-Aldrich, SCC065) were cultured according to the manufacturers protocol. Briefly, cells were maintained in Claycomb (51800C) complete medium (CM) supplemented with 0.1 mM Norepinephrine (Sigma-Aldrich, A0937), 10% HL-1 screened Fetal Bovine Serum (FBS, Sigma, TMS-016) 2 mM L-glutamine (Wisent, 609-065-EL) and 1% Penicillin Streptomycin (P.S, Wisent, 450-200-EL). Culture medium was changed everyday and sub-culture for experiments were maintained in transfection medium (TM), CM without antibiotic.

2.2 Primary Cardiomyocyte Culture (PCM)

Primary cardiomyocytes (PCMs) were isolated from neonatal C57BL/6 mice within 24 h of birth. Neonatal mice were aseptically sacrificed by decapitation according to animal use protocol (AUP 2019-147) approved by the subcommittee of Animal Care and Use of Western University. Hearts were aseptically excised and washed 4 times in cold D-Hanks buffer (Table 2.1) to remove blood or loose debris. Hearts were cut into small pieces, resuspended in 12.5 µg/mL Liberase (Roche, 05401151001) dissolved in D-hanks at 5 mL/10 hearts and incubated for 5 min at 37°C in a water bath. Mixture was mixed with a transfer pipette to stimulate cell release and the supernatant was decanted. Liberase digestion was repeated at 37°C for 15 min 2x, each time hearts were mixed with a transfer pipette to stimulate release and the supernatant was collected into PCM-CM: DMEM/F12 (Wisent, 319-085-CL) supplemented with 15% FBS, 2mM L-glutamine and 1% P.S. The digestion supernatants were spun down, and cells were resuspended in 1 mL/heart in PCM-CM. Cells were plated in a 3.5 cm petri dish and incubated 2 h at 37°C to allow

fibroblasts to attach. After 2 h the medium was collected without disturbing attached cells and the cells were plated 1 heart/well in a 24-well plate pre-coated with 1% gelatin for 2 h at 37°C. Cells were cultured for 3-5 days with fresh medium daily. PCM beating was observed prior to any experiments.

Table 2.1 1x D-Hanks recipe prepared for PCM isolation from neonatal C57/B6 mice.

Component	Concentration
NaCl	140 mM
KCl	5 mM
CaCl ₂	1 mM
MgSO ₄ • 7H ₂ O	0.4 mM
MgCL ₂ • 6 H ₂ O	0.5 mM
Na ₂ HPO ₄ • 2H ₂ O	0.3 mM
KH ₂ PO ₄	0.4 mM
D-Glucose (Dextrose)	6 mM
NaHCO ₃	4 mM

2.3 Ischemia and Reperfusion Injury Model

HL-1 cells were subjected to IRI using GENbag Anaerobic (Biomérieux, 45534) and Belzer UW cold storage solution (Fischer Scientific, NC0624127). Cells in multi-welled plates were cultured in normal cell culture conditions overnight. Cell Culture medium was removed and cells were washed with D-PBS (Gibco, 141190144), incubated with UW solution and placed in a GENbag Anaerobic with an anaerobic indicator

(Biomérieux, 96118). Bags were incubated for 30 min at 37°C to activate anaerobic sachet followed by 24 h cold storage at 4°C to mimic organ preservation. Following hypoxia, cells were reperfused by supplementing UW solution with an equal volume of TM up to 12 h at 37°C. To mimic a similar cell death model in PCMs, 16 h cold storage at 4°C was used to induce hypoxia and 6 h reperfusion at 37°C with full replacement of UW solution with PCM-CM due to the more delicate nature of PCM compared to HL-1.

2.4 CircHIPK3 siRNA mediated knockdown

HL-1 cells were plated between 30,000-80,000 cells/well and incubated over-night (Table 2.2). Cells were transfected with 1 µg:1 µL siRNA-Endofectin mix according to manufacturers protocol. Briefly, GL2 siRNA (5'-CGTACGCGGAATACTTCGA-3', Sigma-Aldrich) or circHIPK3 siRNA (5'-CGCTACTACAGGTATGGCCTCA-3', Sigma-Aldrich) was diluted in equal 50 µL Opti-MEM (Gibco, 31985070) and incubated 5 min at room temperature (RT). Endofectin Max (GeneCopoeia, EF014) was diluted in equal volume Opti-MEM and followed the same incubation. siRNA and endofectin mixtures were combined and incubated for 15 min at RT. Cells were washed with D-PBS and cultured with Opti-MEM where 100 µL siRNA-endofectin mixtures were added for 6 h at 37°C. After 6 h, medium was supplemented with TM and cells were incubated for 24 h – 48 h prior to harvesting for analysis or experiments. Exact amounts and volumes of each reagent can be found in Table 2.2.

Table 2.2 Detailed information and transfection reagent amounts for siRNA mediated knockdown in HL-1 cardiomyocytes.

Transfection Type	Culture Dish	Cell Density	Endofectin (μL): siRNA (μg)	Volume OptiMEM (μL)	Volume TM added after 6h (mL)
siRNA	24 well	10,000/well	0.5:0.5	100	0.3
	12 well	30,000/well	1:1	200	0.8
	6 well	80,000/well	2:2	500	1.5

2.5 Real-time Cell Death using an Incucyte System

After induction of hypoxia, cell death was dynamically monitored during reperfusion from 0 h to 12 h using an incucyte to assess real-time cell death. Briefly, 1 μg/mL Propidium Iodide (PI, Thermo Fisher Scientific, P3566) was added to each well during reperfusion, 9 images of phase and red fluorescent were taken per well each hour at 4x magnification. Red objects indicate PI positive staining of DNA and cell death were counted per well between the 9 images at each interval and plotted against time at each hour to generate cell death curve.

2.6 Cell Apoptosis and Death Quantification by Flow Cytometry

Following experimental endpoint, the culture supernatant was collected in a FACS tube, cells were washed with 500 μL PBS which was also collected. Cells were harvested with 0.05% trypsin for 2 min at 37°C and neutralized with 1 volume CM. Cells were spun down x 500g 5 min at 4°C and washed with 1 mL cold Annexin V binding buffer (BioLegend, 420201) and spun again. Cells were resuspended in 100 μL Annexin V binding buffer containing 2 μL Annexin V APC antibody (BioLegend, 640919) and 5 μL

of 0.5 mg/mL PI and incubated for 15 min at RT in the dark. After incubation cells were diluted with 100 μ L binding buffer and run on a CytoflexS (Beckman Coulter, Pasadena, California, USA) using the following laser gain for the respectively channels: 150 FSC, 150 SSC, 200 APC-A, 5 ECD. Compensation was applied from mixed populations of viable and heat-killed cells at 95°C 5 min.

2.7 RNA Isolation

Total RNA was isolated from cells using QIAzol lysis reagents (Qiagen, 79306). Cells were washed with PBS and QIAzol was added directly to the monolayer. Cells were incubated at RT for 10 min prior to collect with a cell scraper. 1:5 volume chloroform was added to each tube, inverted 6 times and incubated 5 min at RT. Tubes were centrifuged at >18,000g for 15 min at 4°C and the top aqueous layer was removed and placed into a new tube with 1 volume isopropanol, inverted 6 times and incubated 5 min at RT. RNA was pelleted at 18,000g for 10 min at 4°C. Supernatant was decanted and 1 mL 75% cold ethanol was added to wash, tubes were vortexed briefly to displace pellet, and spun again at 18,000g 5 min. The ethanol was decanted, tubes were briefly spun, and the remainder removed by pipette. Pellet was air dried 10-15 min, resuspended in 20-30 μ L RNase-free H₂O (Invitrogen, 10977015) and heated at 55°C for 15 min to dissolve RNA. Concentrated was measured at 260nm using a microvolume spectrophotometer DS-11 (Denovix, Wilmington, Delaware, USA).

2.8 cDNA generation

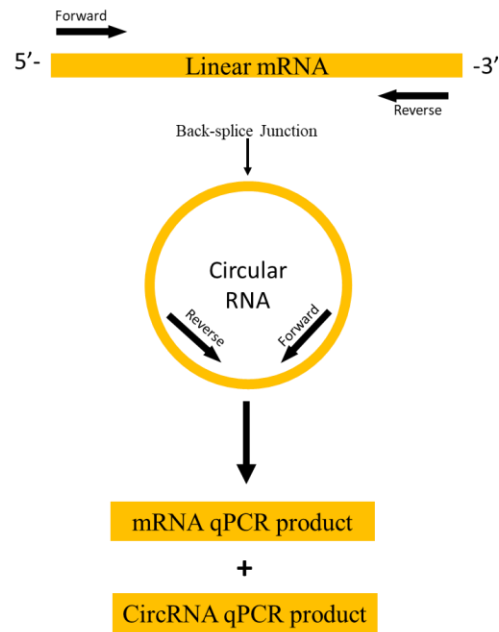
cDNA was generated using One Script Plus cDNA First strand kit (ABM, G236). Briefly, 2 μ g of total RNA was mixed with 1 μ L random hexamer (10 μ M), 1 μ L dNTP (10 μ M)

and diluted to 14.5 μL . Samples were incubated at 65°C for 5 min followed by ice for 2 min. 4 μL 5x buffer was added along with 0.5 μL RNase OUT (40U/ μL) and 1 μL reverse transcriptase enzyme. Samples were incubated at 25°C 10 min, 55°C for 15 min and 85°C 5 min. cDNA was diluted 10x by adding 180 μL RNase Free water.

2.9 Quantitative Polymerase Chain Reaction (qPCR)

qPCR was performed using BrightGreen 2x qPCR mastermix (ABM, mastermix-s) or BlastTaq 2x qPCR mastermix (ABM, G892) in 10 μL reaction. Briefly, 2 μL of diluted cDNA was incubated with 2x qPCR master mix, 200 nM forward/reverse primers, and incubated at 95°C 10 min, 40 cycles of 95°C 15s and 60°C 1 min on a CFX Connect (Bio-rad, Hercules, California, USA). In the case of low gene expression, up to 4 μL diluted cDNA was used in a 20 μL reaction. circHIPK3 was detected using divergent primers (Figure 2.1). A full list of primers used, and their sequences can be found in Table 2.3. To analyse gene expression, the delta-delta Ct method was used with GAPDH or beta-actin acting as a loading control.

Traditional primers



Divergent Primers

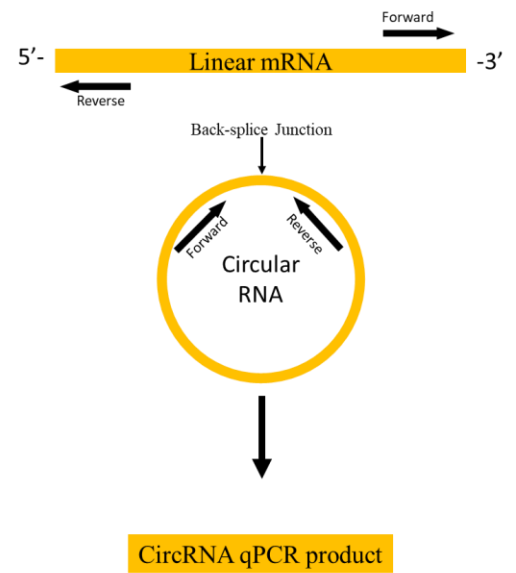


Figure 2.1 Divergent primers and their use to amplify circRNA across their back-splice junction distinguishing them from their linear counterpart and traditional primer design.

Table 2.3 All primers used for qPCR and their sequences from 5' – 3' orientation.

Primer	Sequence
circHIPK3	F: 5'-CATGCTGACCTCAAACCAGA-3'
	F: 5'-ACACAACCGCTTGGCTCTAC-3'
Hipk3	F: 5'-TGTACGTGTTGGGGCACTTA-3'
	F: 5'-CGGTTACAATGCAGCTGAGA-3'
Bax	F: 5'-GGTGACCTGCTTTTTGGCTGt-3'
	R: 5'-TTACGGTCAGGATGGGGTCT-3'
Bak	F: 5'-GGTGACCTGCTTTTTGGCTG-3'
	R: 5'-TTACGGTCAGGATGGGGTCT-3'
Bcl-2	F: 5'-GTGGAGCCGGCGAAATAAA-3'
	R: 5'-TAGATGGCAGGCGTTATCGG-3'
Bcl-XL	F: 5'-CCTTGGATCCAGGAGAACGG-3'
	R: 5'-CGACTGAAGAGTGAGCCCAG-3'
Caspase 3	F: 5'-ATGGGAGCAAGTCAGTGGAC-3'
	R: 5'-GTCCACATCCGTACCAGAGC-3'
Caspase 8	F: 5'-TCAAAGTGCCCTTCCCTGTC-3'
	R: 5'-GCCTCATCAGGCACTCCTTT-3'
Caspase 9	F: 5'-AAGTTTGCCTACCCCCAGTG-3'
	R: 5'-GGTCTCGATGTACCAGGAGC-3'
TNF α	F: 5'-CGTCAGCCGATTTGCTATCT-3'
	R: 5'-CGGACTCCGCAAAGTCTAAG-3'
IL-6	F: 5'-CCGGAGAGGAGACTTCACAG-3'
	R: 5'-GGAAATTGGGGTAGGAAGGA-3'
IL-18	F: 5'-TACCTGTGGACTATCAGACACCT-3'
	R: 5'-GGTTTGAGGCGGCTTTCTTT-3'
GAPDH	F: 5'-GGGGTGAGGCCGGTGCTGAGTAT-3'
	R: 5'-CATTGGGGTAGGAACACGGAAGG-3'
B-actin	F: 5'-CAGCTGAGAGGGAAATCGTG-3'
	R: 5'-CGTTGCCAATAGTGATGACC-3'

2.10 CircHIPK3 primer validation

circHIPK3 primers were validated using RNase R digestion protocol. Briefly, 5 μ g of total RNA was digested with RNase R (ABM, E049) for 3 h at 37°C. Following digestion, a volume representing 1 μ g total RNA was used for cDNA synthesis as

described above. Following cDNA, qPCR was performed as described above for circHIPK3, Hipk3 and GAPDH. A mock digestion containing no RNase R was performed simultaneously to mimic control conditions. $2^{\Delta Ct}$ between circHIPK3 or Hipk3 and mock digestion GAPDH cycling was used to represent enrichment or degradation of RNA levels. qPCR products were then sent for sanger sequencing (Robarts Research Institute, London, ON) to confirm back-splicing products.

2.11 Lactate Dehydrogenase (LDH) Assay

LDH assay was performed using a CytoTox 96 Non-radioactive cytotoxicity assay kit (Promega, G1780). Briefly, supernatant was collected at the desired timepoint from cells following IRI experiments described above. 50 μ L of supernatant was mixed with 50 μ L of CytoTox 96 reagent: substrate mix reconstituted in 12.5 mL of assay buffer, and incubated at room temperature for 30 min. After 30 min 50 μ L of stopping solution was added to each well and the absorbance was measured at 490 nm. Absorbance of treatment groups were compared to normoxia supernatant as control levels of LDH. A blank containing fresh culture medium and a maximum positive control were included to ensure assay functionality.

2.12 Protein Isolation and Western Blotting

Cells were washed and collected in cold PBS, pelleted at 500g for 5 min at 4°C and the supernatant removed. Pellet was resuspended in cold RIPA lysis buffer (Cell signalling, 9806) supplemented with 1 mM PMSF (Cell signalling, 8553S) and incubated on ice for 20 min. Samples were spun at 18,000g for 20 min, the supernatant was collected and 5 μ L was used to determine concentration using a Pierce BCA protein assay (Thermo Scientific, 23225) against a bovine serum albumin (BSA, Amresco, 0332) standard curve.

To allow equal concentration of all samples and a greater amount of protein to be loaded in low-yield samples, 10-20 μg of protein was mixed with 5x volume of cold acetone (Caledon, 1201-2-10) and incubated at -20°C overnight to precipitate proteins. Proteins were pelleted at 18,000g for 10 min, dried, resuspended at 2 $\mu\text{g}/\mu\text{L}$ in 1x loading buffer containing, 10% glycerol, 2% SDS, 0.1 M DTT, 0.01% Bromophenol blue in 0.375 M Tris-HCl, and boiled at 95°C for 5 min. 15 μg protein was loaded per well and run on a 12% polyacrylamide SDS gel at 60V for 30 min followed by 1.5 h at 100V. Transfer was done using a trans-blot TURBO system (Biorad, Hercules, California, USA) according to manufacturer's protocol. Membranes were blocked in 3% fat-free skim milk dissolved in PBST 0.1% tween-20 (Sigma-Aldrich, P9416) for 30 min at RT prior to addition of primary antibody in PBST + 1% BSA overnight at 4°C . A list of primary antibodies and their dilutions can be found in Table 2.4. Membranes were washed for 5 min 3x in PBST at RT prior to addition of secondary antibody, donkey anti-rabbit (Invitrogen, A16023) or goat anti-mouse (Invitrogen, A16066) in PBST, for 1.5 h at RT. Species reactivity and dilution of secondary antibody can be found in table 2.4. Membranes were washed again for 5 min 3x at RT in PBST prior to being exposed to an in-house ECL containing 1.25 mM Luminol (Sigma-Aldrich, A8511), 2 mM 4-Iodophenylboronic acid (Sigma-Aldrich, 471933), 5.4 mM H_2O_2 (Fischer Scientific, H325), in 100 mM Tris-HCl pH 7.2 for 2 min before imaging. Membranes were imaged in a FluoroChem M (Protein Simple, San Jose, California, USA) using chemiluminescence for protein bands and red fluorescence for protein marker. Bands with weak chemiluminescence were visualized using Clarity Max western ECL (Bio-rad, 1705062). After initial detected, membranes were washed 10 min in PBS and stripped using mild-stripping buffer; for 15 min 2x. Membranes were washed in PBS for 10 min 3x and subjected to blocking and immunoblotting again.

Table 2.4 Table of all primary antibodies used and their respective dilution.

Primary Antibody Target and Dilution	Host Species	Company and Catalogue Number	Secondary Antibody Used and Dilution
B-actin (1:1000)	Mouse	Santa Cruz Biotechnology (SC47778)	Goat Anti-Mouse (1:5000)
Caspase 3 (1:1000)	Rabbit	Cell Signalling (9662)	Donkey Anti-Rabbit (1:5000)
Bax (1:1000)	Rabbit	Cell Signalling (2772)	
Bcl-XL (1:1000)	Rabbit	Cell Signalling (2764)	
P-MLKL (1:1000)	Rabbit	Cell Signalling (37333)	
MLKL (1:1000)	Rabbit	Cell Signalling (37705)	

Images were exported and densitometry was done using AlphaView Stand Alone or ImageJ density measurement. Briefly, bands were isolated and chemiluminescent intensity was normalized against B-actin from the same sample. Samples were then normalized against normoxia control bands. Phospho-proteins were normalized against their un-phosphorylated form prior to normalization against their normoxia controls.

2.13 Statistical Analysis

Statistical analysis was performed using GraphPad PRISM version 9.1.1. Students t-test or One-way ANOVA was performed, and data is represented as means \pm SEM of a minimum of three independent experiments (n=3) unless stated.

Chapter 3. Results

3.1 CircHIPK3 expression increases during cardiac IRI

To determine the role of circHIPK3 in cardiac IRI, we used murine cardiomyocyte cell line HL-1 cells and built an *in vitro* IRI model. Using an incucyte system to monitor real-time cell death during reperfusion, we showed that our cold-storage and supplementation model caused HL-1 cells to die in a linear fashion compared to normoxia cells during reperfusion (Figure 3.1B). Using this model, we chose an early injury time point; 4 h, and a later injury time point; 8 h. Using our time points, we determined the expression of circHIPK3 and its parent gene Hipk3 qPCR. We found that circHIPK3 was up regulated at both 4 h and 8 h reperfusion (Figure 3.1C) where Hipk3 mRNA was not changed (Figure 3.1C), showing independent regulation between the circRNA and its home gene in HL-1 cells.

To confirm circHIPK3 expression during IRI, we used primary cardiomyocytes (PCMs) and induced IRI. circHIPK3 showed increased expression during IRI in PCMs (Figure 3.1D). However, Hipk3 mRNA expression was also increased in PCM (Figure 3.1D) indicating independent regulation of circHIPK3 is not clear in primary cells.

To confirm the accuracy of circHIPK3 detection with our divergent primers, RNase R digestion was performed on total RNA. RNase R degrades linear RNA, destroying rRNA and mRNA leaving circRNA untouched. Following mock digestion RNA treatment, cDNA and qPCR for circHIPK3 and Hipk3, the $2^{\Delta Ct}$ of Hipk3 was significantly larger than circHIPK3 (Figure 3.1E) showing higher expression in cells. Following RNase R digestion, there was an increase in $2^{\Delta Ct}$ of circHIPK3 and subsequent decrease in linear Hipk3 (Figure 3.1E). The change in $2^{\Delta Ct}$ represents an enrichment in

CircRNA fractions in total RNA and a decrease in linear mRNA. Sanger sequencing was conducted on qPCR products of circHIPK3 to confirm the existence of the back-splice junction sequence. Sanger sequencing showed the qPCR products matched Hipk3 exon 2 at the back-splice junction (Figure 3.1F), where the 3' end of exon 2 joins the 5' end and is upstream of the 5' end upon amplification with divergent primers (Figure 3.1F).

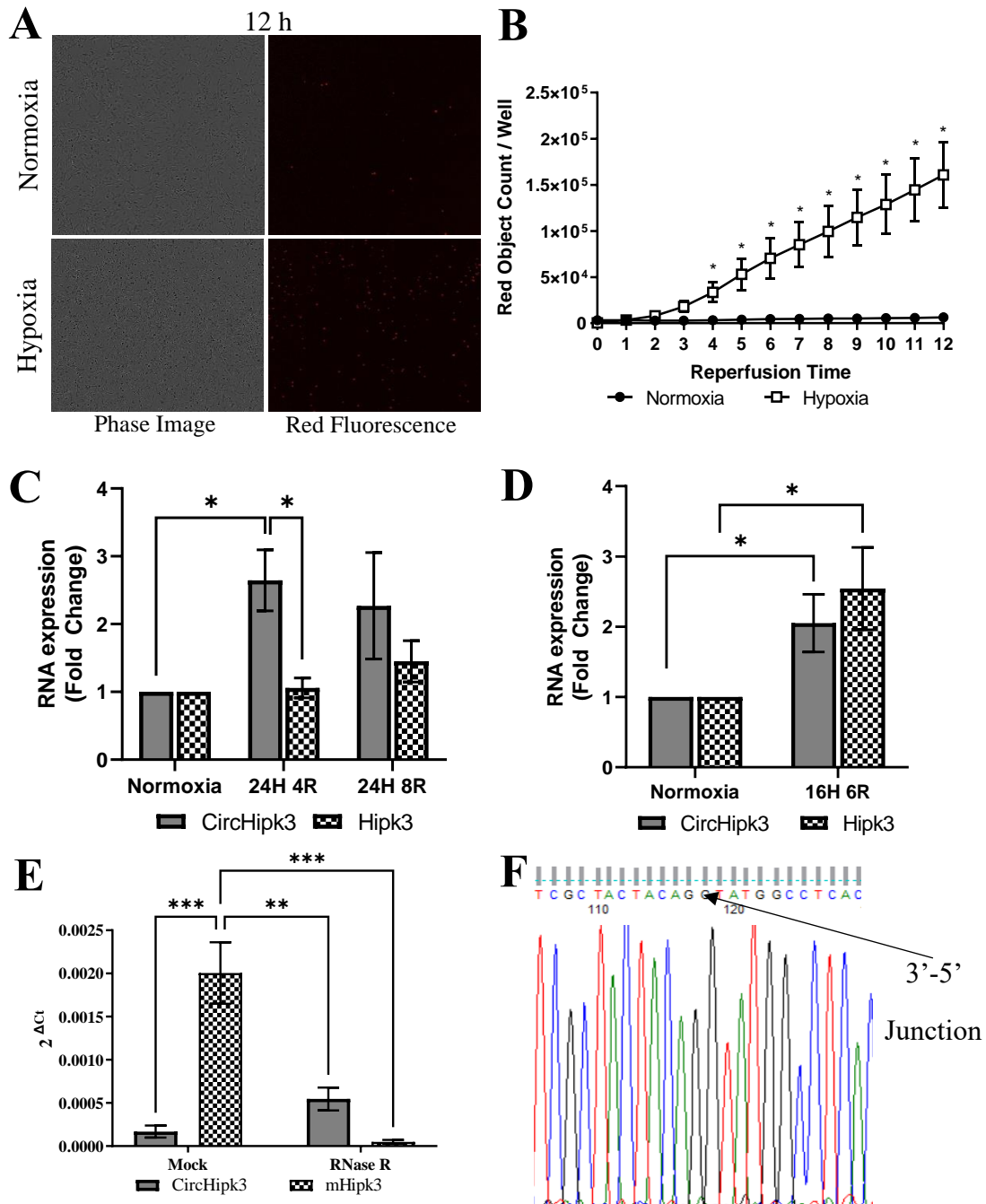


Figure 3.1 Expression of circHIPK3 is increased during IRI. (A/B) Validation of IRI model inducing death, (C) expression of circHIPK3 and Hipk3 following IRI at 4 h and 8 h post reperfusion, (D) circHIPK3 expression in PCM following IRI at 6 h reperfusion, (E) Delta Ct values of circHIPK3 and Hipk3 following RNase R or mock digestion (F) Sanger sequencing of the back-splice sequence from circHIPK3 qPCR products. *= $p < 0.05$, **= $p < 0.01$, ***= $p < 0.001$, ****= $p < 0.0001$.

3.2 CircHIPK3 knockdown prior to IRI leads to increased cell death

To determine the role of circHIPK3 expression in cardiac IRI, we performed a loss-of-function assay through RNA interference. An siRNA (circHIPK3 siRNA) evenly spanning the back-splice junction of circHIPK3 was first designed, synthesized, and validated. HL-1 cells were transfected with circHIPK3 siRNA, or control GL2 siRNA and qPCR was conducted to measure the expression of circHIPK3 and Hipk3. It shows that circHIPK3 siRNA achieved more than 60% knockdown of circHIPK3 48 h after transfection but had no effect on Hipk3 mRNA levels compared to GL2 siRNA (Figure 3.2A).

Next, we determined the effect of circHIPK3 knockdown on IRI. HL-1 cells were transfected with circHIPK3 siRNA 24 h prior to a 24 h cold ischemia (hypoxia) environment. Real time cell death was measured to evaluate IRI, using an incucyte system. We found circHIPK3 knockdown prior to IRI leads to significantly increased cell death during reperfusion (Figure 3.2B) when compared to GL2 siRNA. We found no difference in cell death between GL2 and circHIPK3 siRNA following cold storage, with a steep increase in red PI positive cells which are dead cells in circHIPK3 siRNA groups beginning 4 h post reperfusion (Figure 3.2B). There were also no observed changes in cell morphology prior to reperfusion (Figure 3.2C). Collectively, this indicates that the difference in cell viability is driven during the reperfusion phase.

Lactate Dehydrogenase (LDH) is commonly used as a biomarker for cardiac injury, including those involving ischemia induced damage. To further assess damage to our cells, we measured the relative free LDH in the supernatant of at 4 h reperfusion. We found that cell supernatant with GL2 siRNA had significantly increased LDH relative to

normoxia (Figure 3.2D), and that circHIPK3 siRNA groups had significant increased LDH compared to normoxia and GL2 siRNA (Figure 3.2D), indicating increased cellular damage and release of LDH.

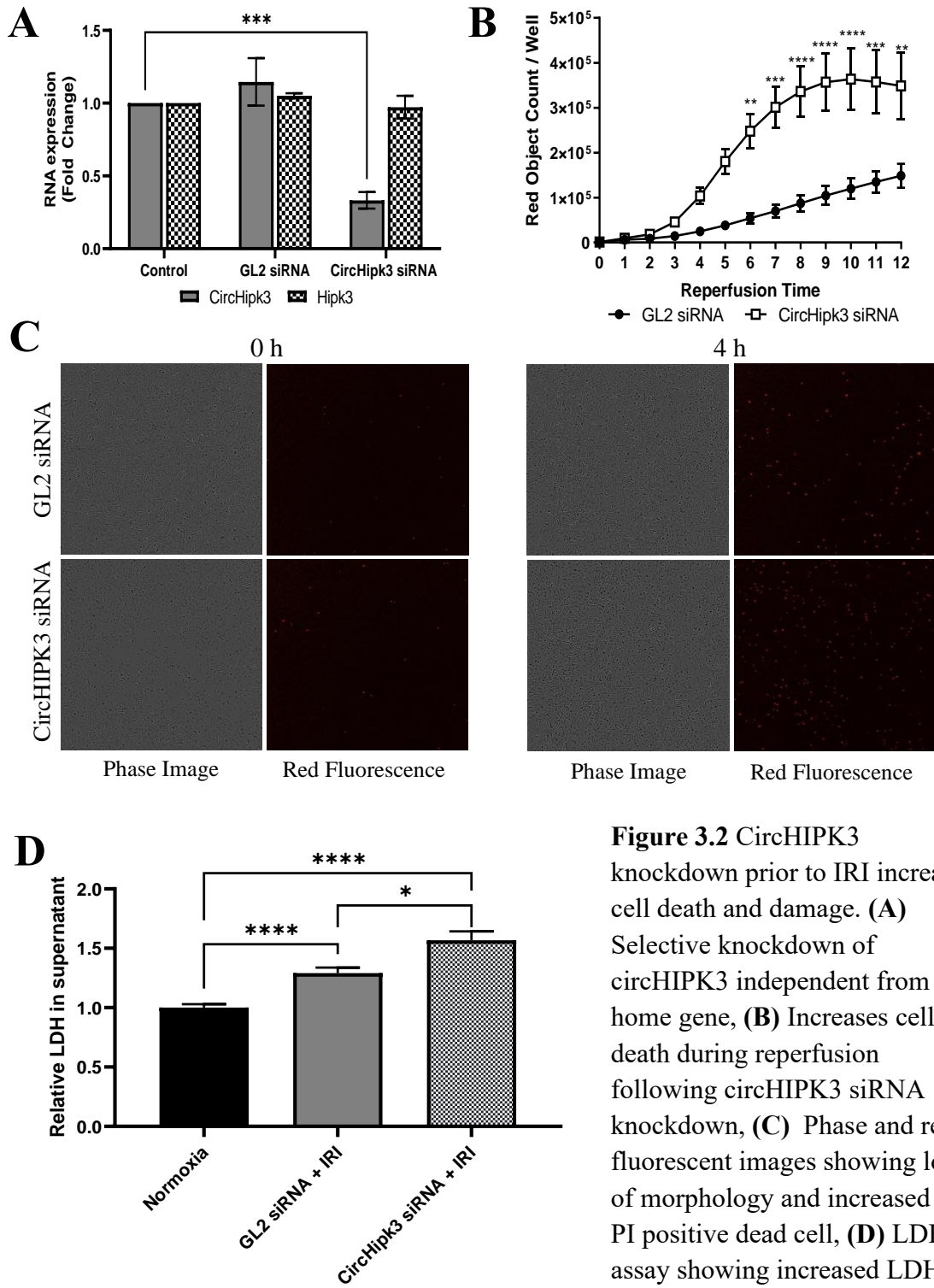


Figure 3.2 CircHIPK3 knockdown prior to IRI increases cell death and damage. **(A)** Selective knockdown of circHIPK3 independent from home gene, **(B)** Increases cell death during reperfusion following circHIPK3 siRNA knockdown, **(C)** Phase and red fluorescent images showing loss of morphology and increased red PI positive dead cell, **(D)** LDH assay showing increased LDH in supernatant indicating cellular damage and death. *= $p < 0.05$, **= $p < 0.01$, ***= $p < 0.001$, ****= $p < 0.0001$.

3.3 CircHIPK3 knockdown leaves cells vulnerable to IRI

To determine the mechanism behind circHIPK3 knockdown induced death in IRI, we transfected HL-1 cells with circHIPK3 siRNA for 48 h and analyzed pro- and anti-apoptotic gene expression. First, we analyzed mitochondrial based targets Bax, Bak, Bcl-2 and Bcl-XL. circHIPK3 knockdown for 48 h led to a significant increase in pro-apoptotic Bax gene in HL-1 cells (Figure 3.3A) and an increase in Bcl-2, a pro or anti-apoptotic gene (Figure 3.3A). circHIPK3 knockdown had no effect on Bak or BclXL (Figure 3.3A). Second, we investigated downstream apoptotic caspases 3, 8 and 9. Our results show that CircHIPK3 knockdown induced a significant increase in caspase 3, caspase 8, and caspase 9 relatively to GL2 siRNA (Figure 3.3B). However, GL2 siRNA was slightly down regulated compared to control cells. This is likely contributed to the slight protective effect we observed from long-term culture with Opti-MEM in HL-1 cells. To distinguish between apoptotic and necrotic cell death during IRI, we used Annexin V and PI staining to identify phosphatidyl-serine positive cells in early and late stage apoptosis using flow cytometry. We found that circHIPK3 silenced cells showed an increase in Annexin V positive staining at both 4 h and 8 h reperfusion, compared to normoxia and GL2 control (Figure 3.3C) and the percentage of Annexin V positive cells was increased in GL2 siRNA transfected cells compared to normoxia (Figure 3.3C). A similar trend was observed in PI staining, where GL2 and circHIPK3 siRNA groups had increased PI positive cells at 4 h and 8 h compared to normoxia (Figure 3.3D) and circHIPK3 siRNA exacerbated cell death compared to GL2 siRNA at 8 h only (Figure 3.3D). Double positive Annexin V and PI cells indicating late-stage apoptosis had no significant change at 4 h reperfusion (Figure 3.3E) and only circHIPK3 siRNA group showed a significant increase in double positive cells at 8 h reperfusion (Figure 3.3E).

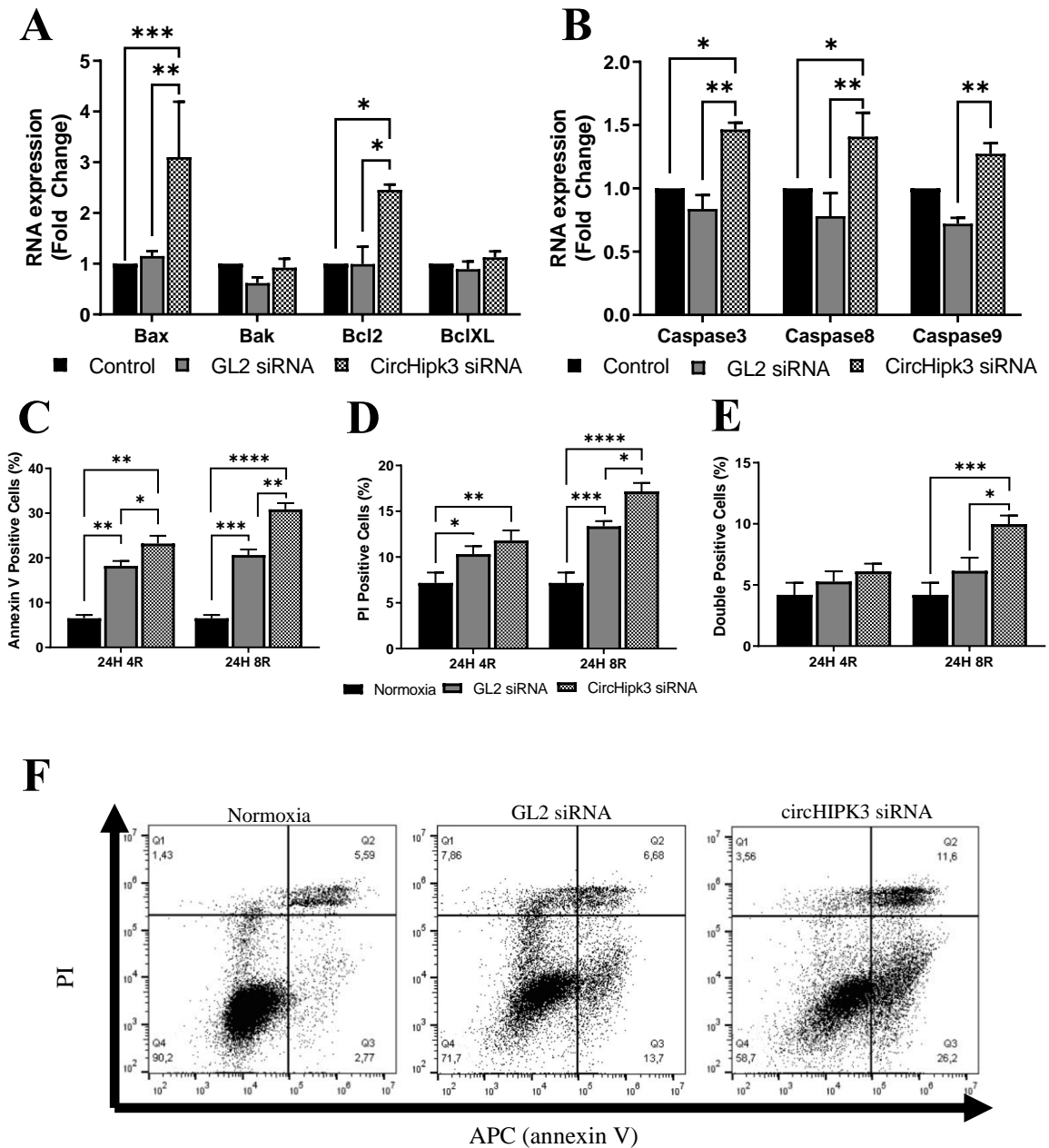


Figure 3.3 CircHIPK3 knockdown leaves cell vulnerable to apoptosis. (A/B) 48 h knockdown of circHIPK3 leads to increase in proapoptotic gene mRNA levels. circHIPK3 knockdown leads to increase annexin V (C), PI (D) and double stained (E) positive cells at 4 h and 8 h reperfusion. (F) Quad plot showing PI vs annexin V staining following 8 h reperfusion. *= $p < 0.05$, **= $p < 0.01$, ***= $p < 0.001$, ****= $p < 0.0001$.

3.4 CircHIPK3 knockdown exacerbates apoptosis and necroptosis during IRI

We previously showed that circHIPK3 knockdown leaves cells vulnerable to IRI through promoting apoptosis. To further investigate the mechanism of injury during IRI, we performed siRNA mediated knockdown of circHIPK3 prior to IRI, followed by RNA collection at 4 h reperfusion. circHIPK3 siRNA successfully downregulated circHIPK3 after IRI while GL2 siRNA showed increase in circHIPK3 expression. (Figure 3.4A). We detected a small decrease in Hipk3 expression in GL2 siRNA transfected samples although not significant (Figure 3.4A). There was no significant change in Hipk3 expression among the groups (Figure 3.4A). Similar to 48 h siRNA treatment without IR, we found exacerbated Bax expression in circHIPK3 knockdown IRI group compared to GL2 siRNA IRI group and normoxia (Figure 3.4B). Bax expression in GL2 siRNA groups was significantly increased compared to normoxia (Figure 3.4B), indicating that IRI further exacerbated Bax mRNA expression. Bak mRNA expression remained unchanged in both IRI groups (Figure 3.4B). We saw a similar trend at the protein level of Bax (Figure 3.4D). Compared to normoxia, GL2 and circHIPK3 siRNA IRI groups both induced Bax protein levels (Figure 3.4F), but no significant difference in protein express was detected between the two groups (Figure 3.4F). Bcl-2 mRNA levels following IRI shared an identical trend to 48 h siRNA transfection. circHIPK3 siRNA group following IRI induced Bcl-2 mRNA expression similar to siRNA alone (Figure 3.3A & Figure 3.4B), but GL2 siRNA had no change (Figure 3.4B), indicating that Bcl-2 expression increase is driven by circHIPK3 knockdown. Bcl-XL mRNA expression was unchanged in 48 h siRNA groups. During IRI, Bcl-XL mRNA shows decreased expression in circHIPK3 siRNA IRI group (Figure 3.4B) compared to GL2 siRNA IRI

and normoxia groups. Bcl-XL mRNA showed no change in response to siRNA knockdown, yet the absence of loss in BclXL mRNA expression in GL2 siRNA IRI groups suggests decreased mRNA is not exclusively driven by IRI. At the protein level, we detected no change in Bcl-XL in GL2 or circHIPK3 siRNA groups compared to normoxia (Figure 3.4).

Caspase 3 and 9 showed no increase in mRNA expression in GL2 or circHIPK3 siRNA IRI groups compared to normoxia (Figure 3.4C). Although no change was observed at the mRNA level, caspase 3 protein showed a significant increase in cleaved caspase 3 in both GL2 and circHIPK3 siRNA groups (Figure 3.4D-E). circHIPK3 siRNA group showed higher amount of cleaved caspase 3 than GL2 siRNA, although the difference was not significant (Figure 3.4E). Caspase 8 showed increased mRNA levels in both GL2 and circHIPK3 siRNA groups, but no difference between them (Figure 3.4C).

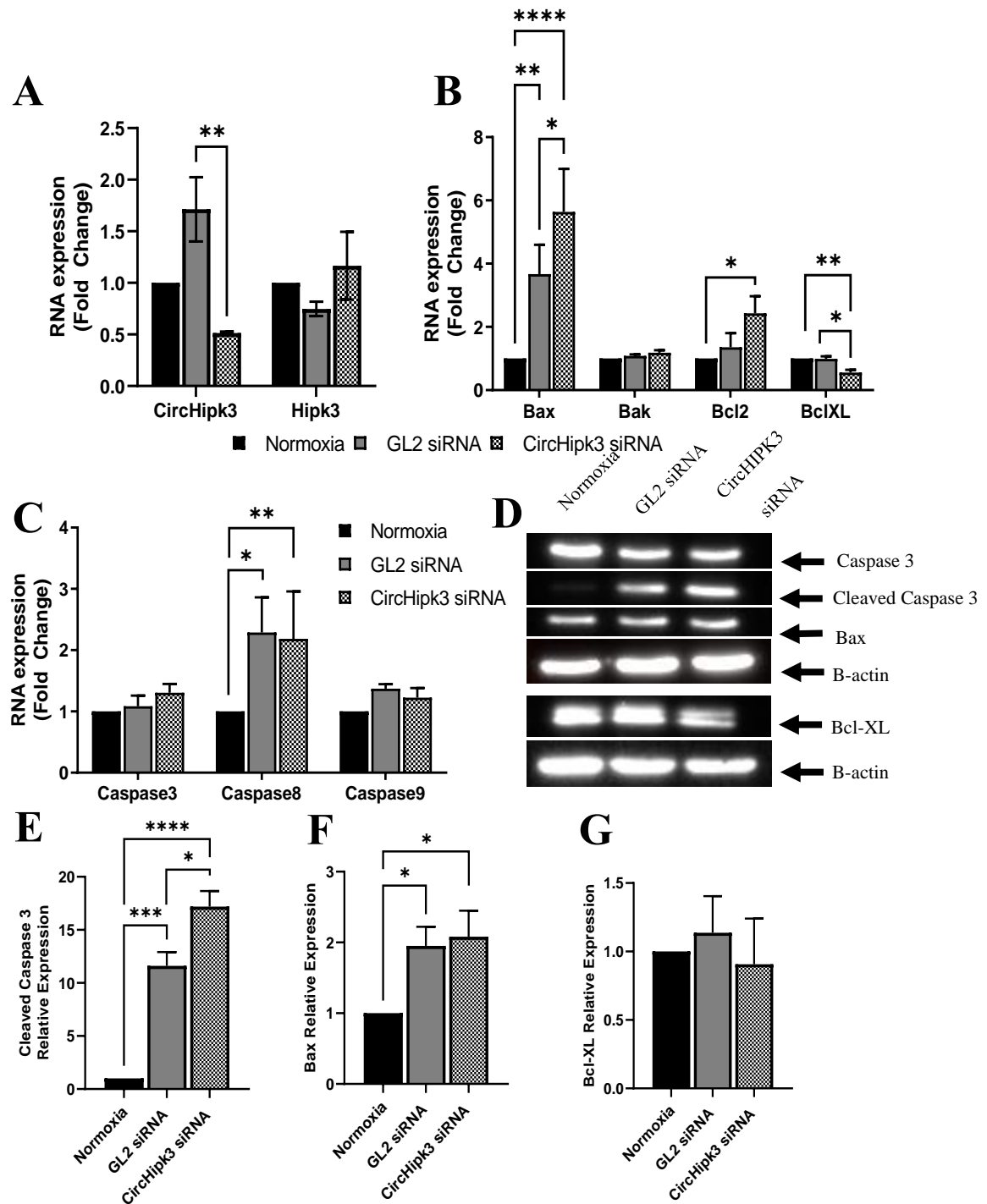


Figure 3.4 CircHIPK3 knockdown exacerbates cell death through activation of apoptosis. (A) qPCR showing circHIPK3 expression remains knocked down after siRNA and IRI compared to GL2 siRNA. circHIPK3 knockdown exacerbates mitochondrial proapoptotic and suppresses anti-apoptotic (B) and increases caspase (C) mRNA levels. CircHIPK3 knockdown exacerbates cleaved caspase 3 (D-E) but has no effect on bax (D,F) or Bcl-XL expression (D,G) * $p < 0.05$, ** $p < 0.01$, *** $p < 0.001$, **** $p < 0.0001$.

Necroptosis exists as a pro-inflammatory cell death mechanism during IRI. To investigate the involvement of necroptosis, we performed western blotting for P-MLKL. Our results show that P-MLKL was up-regulated during IRI in both siRNA groups (Figure 3.5A-B) and exacerbated in circHIPK3 siRNA compared to GL2 siRNA (Figure 3.5A-B). These results suggest that circHIPK3 knockdown exacerbates necroptosis cell death during IRI.

To further investigate the inflammatory response in cells, we measured TNF α , IL-6 and IL-18 mRNA levels. TNF α showed a significant increase in both GL2 and circHIPK3 siRNA compared to normoxia (Figure 3.5C). TNF α mRNA levels in circHIPK3 siRNA IRI group slightly increased compared to GL2 siRNA group but the difference was not significant. IL-6 and IL-18 both showed increase in both GL2 siRNA and circHIPK3 siRNA compared to normoxia (Figure 3.5C), with no difference in IL-18 mRNA levels between the two groups. We did observe a decrease in IL-6 mRNA levels in circHIPK3 siRNA groups compared to GL2 siRNA although it was not significant (Figure 3.5C). Overall, our results suggest circHIPK3 knockdown induces cell death through exacerbation of both apoptosis and necroptosis.

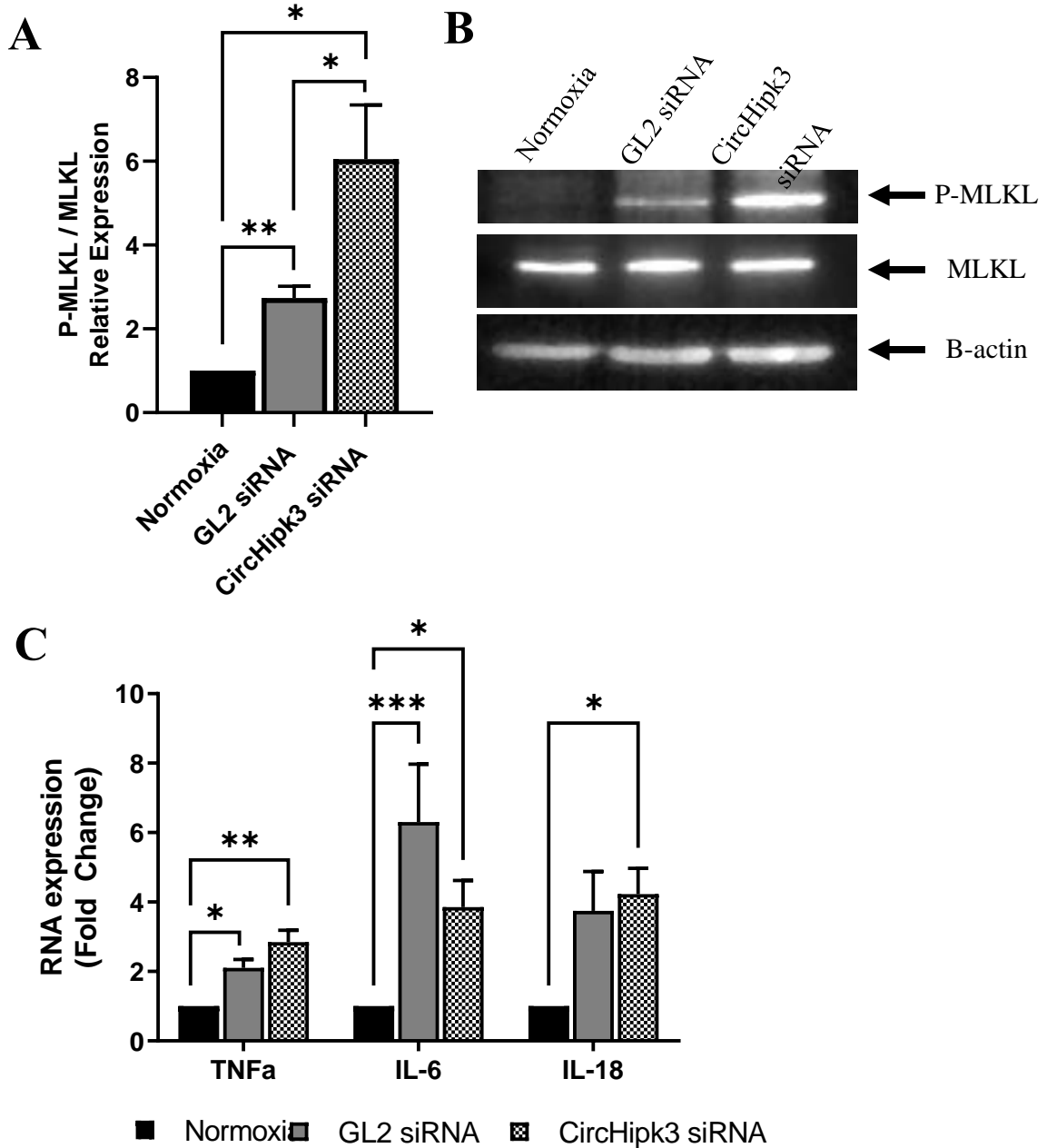


Figure 3.5 CircHIPK3 knockdown exacerbates necroptosis during IRI (A-B) circHIPK3 siRNA exacerbates MLKL phosphorylation during IRI, (C) qPCR quantification of pro-inflammatory mRNA following IRI. $*=p<0.05$, $**=p<0.01$, $***=p<0.001$, $****=p<0.0001$.

Chapter 4. Discussion

4.1 CircHIPK3 expression increases in myocardial IRI

The exact role of circHIPK3 in IRI remains controversial, with some studies suggesting knockdown protects against IRI^{82,83}, while others suggest silencing aggravates myocardial IRI⁸⁴⁻⁸⁶. Due to the differences in cell lines, IRI models and the specific pathway of IRI investigated, it is nearly impossible to compare these studies to form a consensus. Regardless of the affected pathways and consequential pathologies, it is clear that circHIPK3 expression is induced by IRI as reported by all studies, which is consistent with our findings.

Our results showed that following cold-storage cardiac IRI, circHIPK3 expression is increased approximately ~2.5-fold in HL-1 cardiomyocytes in early-stage reperfusion at 4 h and although not significant, to a lesser extent increased in later injury of 8 h. These results are consistent with previous studies showing circHIPK3 is up regulated in cardiac hypoxia and reoxygenation (H/R) models recently published⁸²⁻⁸⁶. We confirmed the expression of circHIPK3 in a PCM based model and found significant increase as well of ~2-fold at 6 h. Previously it was shown that c-myc can bind to the Hipk3 gene promoter and increase circHIPK3 expression driven by high ROS. Although we do not confirm c-myc driven expression of circHIPK3 here, in IRI it is known that ROS sharply increase indicating c-myc is likely a contributing factor⁷². However, our results also showed differential expression of circHIPK3 and Hipk3 during IRI in HL-1 cells, something not investigated by other studies. The observed differential expression suggests the c-myc driven expression is only part of the story, as we see selective back-splicing events to generate circHIPK3 and not Hipk3 mRNA levels, indicating that the splicing mechanism

or Hipk3 negative feedback may also be influenced during IRI in HL-1 cardiomyocytes. We confirmed the increase of circHIPK3 in PCM model however, we did not see the same differential expression of circHIPK3 vs. Hipk3. Although we did not see the same level of differential expression between circHIPK3 and Hipk3 in PCM, this could be contributed to differences in our models. Hipk3 acts as a protein kinase preventing Fas/FADD activation, key components in the extrinsic apoptotic signalling cascade. In our PCM model, we replace UW solution fully and reperfuse with complete medium only. This puts emphasis on ROS generation as the acidity in the solution and lactate build up is more readily cleared, thus it is possible to have low levels of TNF α and reduced extrinsic activation. Due to increased ROS generation, c-myc activation and reduction in extrinsic apoptosis, there may be less negative feedback on Hipk3 expression and a shift in splicing. However, there is currently no evidence suggesting a mechanism or regulation of differential expression between circHIPK3 and Hipk3 and therefore studies must be conducted to elucidate this mechanism.

4.2 CircHIPK3 knockdown leads to increased cell death during IRI

Our IRI model showed increasing cell death in a linear fashion during reperfusion. Upon selective knockdown of circHIPK3 without silencing effects on Hipk3, we showed a significant increase in cell death during IRI. The difference in cell death was only visible starting at 4 h reperfusion as no difference was observed during hypoxia, indicating an apoptotic mechanism as opposed to necrosis. Our dynamic monitoring of cell death not only showed accelerated cell death during reperfusion, but the PI positive dot count and images suggest that after 8 h we had near complete cell death in the entire population, compared to <50% in our GL2 siRNA groups. Our flow cytometry data

showed significant increase in Annexin V positive cells compared to GL2 siRNA following IRI at both 4 h and 8 h. The significant differences observed are consistent with our incuocyte data suggesting increased cell death during IRI and indicates increased apoptosis, as Annexin V binds to phosphatidyl serine, a strong indicator of apoptosis. However, we did not observe or record > 40% of Annexin v positive cells. In addition, our forward and side scatter gating suggest that not all cells experience high side scatter, typically indicative of death, are annexin V positive. This suggests that although apoptosis is exacerbated, there may be other mechanism of death at work.

4.3 CircHIPK3 as a suppressor of apoptosis

To investigate the observed increase in cell death during IRI after circHIPK3 knockdown, we first looked to determine the effects of circHIPK3 knockdown on pro/anti apoptotic genes. We found that 48 h knockdown induced Bax and Bcl-2 mRNA expression significantly compared to GL2 siRNA. Although we did not observe any significant cell death upon transfection, this increase in expression indicates that although cells are not executing apoptosis, they are primed for the signalling cascade to occur and at a quicker rate. Increased Bax and Bcl-2 mRNA expression supports formation of the mPTP during high levels of ROS, exacerbating the intrinsic apoptotic pathway during IRI^{29,87}. The increase in caspase 3, 8 and 9 mRNA observed in cells following siRNA treatment further supports this theory. The increase in caspase 9, being the final step in intrinsic apoptosis, would increase the extent of executor caspase activation. Upon mPTP formation and cytochrome C release, an increase in caspase 9 would result in increased caspase 3 activation and subsequent apoptosis. The increase in caspase 8 suggests that the extrinsic pathway is also exacerbated by circHIPK3 knockdown, as caspase 8 is the final activator

for extrinsically stimulated apoptosis and leads to caspase 3 activation^{29,87}. Collectively, this data along with the increase in caspase 3 mRNA, suggests that circHIPK3 knockdown primes both apoptotic pathways for activation and decreases the stress threshold required for activation.

4.4 CircHIPK3 knockdown promotes apoptosis through intrinsic signalling

It has been previously reported that circHIPK3 silencing induced increased apoptosis and abolished protective effects during IRI^{84,85} and our knockdown studies confirmed the cells are more prone to apoptotic following circHIPK3 silencing. During IRI, we observed that these trends were maintained, especially with Bax expression being further exacerbated. As Bax mRNA levels rise during IRI in GL2 siRNA, we saw a concurrent rise in circHIPK3 siRNA groups indicating that it is the silencing driving this expression. Although no further exacerbation in Bcl-2 was observed, we observed a decrease in Bcl-XL mRNA levels in circHIPK3 siRNA groups. The decrease in Bcl-XL mRNA levels was not observed during knockdown alone and is likely a factor of the increased apoptosis we observe. Essentially, as the cell commits to apoptosis and mPTP formation through Bax and Bcl-2 family members, the anti-apoptotic bcl-2 membranes such as Bcl-XL will receive a negative feedback loop to decrease in expression^{32,34,87}. At the protein level we did not observe differences in Bax expression between GL2 and circHIPK3 siRNA groups nor did we observe any difference in Bcl-XL. Although no change in protein expression was observed, this does not directly represent the amount of mPTP formed. Since Bax expression was induced by circHIPK3 knockdown, if levels of Bax were increased prior to IRI, this would induce quicker mPTP formation and apoptosis as

observed. However, studies involving mPTP formation under IRI following circHIPK3 knockdown would be required to confirm this mechanism of action.

In addition to intrinsic apoptotic activation, we see increases in caspase 8 mRNA levels in both siRNA groups compared to normoxia group. Although we see activation of extrinsic apoptosis pathway, we do not see differences in caspase 8 mRNA between siRNA groups. During knockdown in absence of IRI, we saw increase in caspase 3, 8 and 9 mRNA levels, however during IRI we only observed changes in caspase 8 mRNA. It is possible the increase in caspase mRNA levels following knockdown is a consequence of long-term silencing. During our knockdown studies we performed 48 h treatment as opposed to 24 h prior to IRI. During 48 h knockdown, the increased Bax expression may lead to slight mPTP formation, which result in leakage of ROS and subsequent activation of pro-apoptotic stimuli. This leakage may not be sufficient to activate apoptosis but may be responsible for the increase in pro-apoptotic mRNA expression. TNF α is a potent activator of extrinsic apoptosis^{29,31,35}. During IRI there was no significant difference in TNF α expression between siRNA groups, indicating that exacerbated extrinsic apoptosis pathway is unlikely in this model as suggested by our caspase 8 mRNA results.

Taken together, this data suggests that circHIPK3 siRNA exacerbates intrinsic apoptosis signalling through increasing Bax and Bcl-2 expression, resulting in increased caspase 3 activation compared to control siRNA. Further studies investigating the effects of circHIPK3 on mPTP formation, mitochondrial stability and cytochrome C release are needed to confirm these findings.

4.5 CircHIPK3 knockdown leads to increased necroptosis

Traditionally, necroptosis and extrinsic apoptosis are antagonistic, where caspase mediated cleavage of RIP1 and RIP3 results in inhibited necrosome formation and P-MLKL formation. However, in our studies we show exacerbation of both P-MLKL and extrinsic apoptosis during IRI. Additionally, P-MLKL is enhanced following circHIPK3 siRNA indicating that knockdown promotes necroptosis. The exacerbation of necroptosis following enhanced caspase 8 mRNA is a unique finding and represents a possible role of circHIPK3 in P-MLKL formation simultaneously with apoptosis. Although necroptosis is known to work through the RIP1/RIP3 pathway where caspase 8 activation can mediate its formation, it is presumed there are other checkpoints in place that could inhibit caspase 8 degradation or promote necrosome formation that are not understood which circHIPK3 may play a role in.

4.6 Clinical Implications and Future

circHIPK3 has been gaining attention and showing promise as a regulator of disease in the past few years, with over 40 publications across multiple disciplines focusing on the role of circHIPK3 expression in disease. The clinical relevance of circHIPK3 expression has begun to be investigated in cancer and diabetes, where circHIPK3 expression is compared against disease prognosis and physiological features^{71,74}, but the role of circHIPK3 in IRI at the clinical or *in vivo* level has yet to be investigated. In the current state, due to the controversial role of circHIPK3 expression on cell viability, the use of circHIPK3 as a biomarker is unlikely. However, the increase in circHIPK3 expression could potentially be used to determine if IRI occurs, as circHIPK3 expression is likely driven by ROS and c-myc activation, a constant in IRI. Whether or

not the expression of circHIPK3 could be proportionate to ROS and extent of injury remains unknown.

At the current stage, circHIPK3 has no clear role in IRI at the clinical level however, the data of newly published papers suggest it may have a future. The role of circHIPK3 regulation in IRI has shown to have large implications for cellular viability *in vitro*. Our own data supports this claim where knockdown leads to almost complete cell death very quickly compared to GL2 siRNA. The large effects we see of circHIPK3 on cell death are indicative of a potential role as a strong therapeutic target for IRI. However, further studies elucidating the mechanism of circHIPK3 function and clinical applicability, such as correlation studies between circHIPK3 expression and IRI severity are required to determine circHIPK3 efficacy as a therapeutic target.

4.7 Conclusion and Future directions

In conclusion, our results demonstrated that IRI up-regulates circHIPK3 expression in cardiac cells and circHIPK3 siRNA increases cell death during IRI through exacerbation of necroptosis and intrinsic apoptotic pathways, leading to increase P-MLKL phosphorylation and caspase 3 activation. Our results are in accordance with previous reports suggesting circHIPK3 expression in IRI provides protective effects and that the cellular response to increase circHIPK3 is potentially protective. Our study shows strong evidence of gene regulation and pathway activation however, we do not show evidence of mPTP formation or necrosome formation. Therefore, we cannot conclude whether P-MLKL formation is caused by standard RIP signalling or an alternative mechanism. In addition, we did not observe Bax protein expression experiments following 48 h knockdown and can therefore not confirm whether Bax protein levels are

increased prior to IRI or if the increase in protein is stimulated by IRI alone. In our study we did not show over-expression of circHIPK3 being protective as others have.

Overall, future studies further investigating the mechanism of action through apoptosis and necroptosis must be confirmed as well as using a synergistic heart transplant animal model to confirm deleterious or protective effects of circHIPK3 during cardiac IRI.

Chapter 5. References

1. Table 1 - Ranking and number of deaths for the 10 leading causes of death, Canada, 2000 and 2009. <https://www150.statcan.gc.ca/n1/pub/84-215-x/2012001/table-tableau/tb1001-eng.htm>.
2. Report from the Canadian Chronic Disease Surveillance System: Mental Illness in Canada, 2015 - Canada.ca. <https://www.canada.ca/en/public-health/services/publications/diseases-conditions/report-canadian-chronic-disease-surveillance-system-mental-illness-canada-2015.html>.
3. Isaac, D. *et al.* Cardiac Transplantation: Eligibility and Listing Criteria in Canada 2012 Cardiac Transplantation: Eligibility and Listing Criteria in Canada. (2011).
4. Annual Statistics on Organ Replacement in Canada: Dialysis, Transplantation and Donation, 2009 to 2018. (2019).
5. Carden, D. L. & Granger, D. N. Pathophysiology of ischaemia-reperfusion injury. *Journal of Pathology* vol. 190 255–266 (2000).
6. Braunwald, E. & Kloner, R. A. The stunned myocardium: Prolonged, postischemic ventricular dysfunction. *Circulation* vol. 66 1146–1149 (1982).
7. Hoy, S. & Frisbee, J. Common postoperative heart transplant complications. *Crit. Care Nurs. Q.* **41**, 383–388 (2018).
8. Raedschelders, K., Ansley, D. M. & Chen, D. D. Y. The cellular and molecular origin of reactive oxygen species generation during myocardial ischemia and reperfusion. *Pharmacology and Therapeutics* vol. 133 230–255 (2012).

9. Worthley, S. G., Osende, J. I., Helft, G., Badion, J. J. & Fuster, V. Coronary artery disease: pathogenesis and acute coronary syndromes - PubMed. *Mt Sinai J Med* **68**, 167–181 (2001).
10. Granger, D. N. & Kvietys, P. R. Reperfusion injury and reactive oxygen species: The evolution of a concept. *Redox Biol.* **6**, 524–551 (2015).
11. Wu, M. Y. *et al.* Current Mechanistic Concepts in Ischemia and Reperfusion Injury. *Cellular Physiology and Biochemistry* vol. 46 1650–1667 (2018).
12. Costantini, C. *et al.* Revascularization after 3 hours of coronary arterial occlusion: Effects on regional cardiac metabolic function and infarct size. *Am. J. Cardiol.* **36**, 368–384 (1975).
13. Bolooki, H. Myocardial revascularization after acute infarction. *Am. J. Cardiol.* **36**, 395–406 (1975).
14. Reimer, K. A., Murry, C. E., Yamasawa, I., Hill, M. L. & Jennings, R. B. Four brief periods of myocardial ischemia cause no cumulative ATP loss or necrosis. *Am. J. Physiol. - Hear. Circ. Physiol.* **251**, (1986).
15. Southard, J. H. *et al.* Important components of the UW solution. *Transplantation* **49**, 251–257 (1990).
16. Rosenfeldt, F. L. *et al.* Comparison of UW solution and St. Thomas' solution in the rat: Importance of potassium concentration. *Ann. Thorac. Surg.* **61**, 576–584 (1996).
17. Horwitz, L. D., Wallner, J. S., Decker, D. E. & Buxser, S. E. Efficacy of lipid

- soluble, membrane-protective agents against hydrogen peroxide cytotoxicity in cardiac myocytes. *Free Radic. Biol. Med.* **21**, 743–753 (1996).
18. Bagheri, F. *et al.* Reactive oxygen species-mediated cardiac-reperfusion injury: Mechanisms and therapies. *Life Sciences* vol. 165 43–55 (2016).
 19. Salem, J. E., Saidel, G. M., Stanley, W. C. & Cabrera, M. E. Mechanistic model of myocardial energy metabolism under normal and ischemic conditions. *Ann. Biomed. Eng.* **30**, 202–216 (2002).
 20. Han, D., Williams, E. & Cadenas, E. Mitochondrial respiratory chain-dependent generation of superoxide anion and its release into the intermembrane space. *Biochem. J.* **353**, 411–416 (2001).
 21. Chance, B., Sies, H. & Boveris, A. Hydroperoxide metabolism in mammalian organs. *Physiol. Rev.* **59**, 527–605 (1979).
 22. Turrens, J. F., Alexandre, A. & Lehninger, A. L. Ubisemiquinone is the electron donor for superoxide formation by complex III of heart mitochondria. *Arch. Biochem. Biophys.* **237**, 408–414 (1985).
 23. Han, D., Antunes, F., Canali, R., Rettori, D. & Cadenas, E. Voltage-dependent anion channels control the release of the superoxide anion from mitochondria to cytosol. *J. Biol. Chem.* **278**, 5557–5563 (2003).
 24. Chen, Q., Vazquez, E. J., Moghaddas, S., Hoppel, C. L. & Lesnefsky, E. J. Production of reactive oxygen species by mitochondria: Central role of complex III. *J. Biol. Chem.* **278**, 36027–36031 (2003).

25. Pasdois, P., Parker, J. E., Griffiths, E. J. & Halestrap, A. P. The role of oxidized cytochrome c in regulating mitochondrial reactive oxygen species production and its perturbation in ischaemia. *Biochem. J.* **436**, 493–505 (2011).
26. Arroyo, C. M. *et al.* Spin trapping of oxygen and carbon-centered free radicals in ischemic canine myocardium. *Free Radic. Biol. Med.* **3**, 313–315 (1987).
27. Bolli, R. *et al.* Direct evidence that oxygen-derived free radicals contribute to postischemic myocardial dysfunction in the intact dog. *Proc. Natl. Acad. Sci. U. S. A.* **86**, 4695–4699 (1989).
28. Sawicki, G. *et al.* Degradation of myosin light chain in isolated rat hearts subjected to ischemia-reperfusion injury: A new intracellular target for matrix metalloproteinase-2. *Circulation* **112**, 544–552 (2005).
29. Elmore, S. Apoptosis: A Review of Programmed Cell Death. *Toxicologic Pathology* vol. 35 495–516 (2007).
30. Igney, F. H. & Krammer, P. H. Death and anti-death: Tumour resistance to apoptosis. *Nature Reviews Cancer* vol. 2 277–288 (2002).
31. Walsh, C. M. Grand challenges in cell death and survival: Apoptosis vs. necroptosis. *Front. Cell Dev. Biol.* **2**, (2014).
32. Di Lisa, F., Canton, M., Menabò, R., Kaludercic, N. & Bernardi, P. Mitochondria and cardioprotection. *Heart Fail. Rev.* **12**, 249–260 (2007).
33. Di Lisa, F., Kaludercic, N., Carpi, A., Menabò, R. & Giorgio, M. Mitochondrial pathways for ROS formation and myocardial injury: The relevance of p66Shc and

- monoamine oxidase. *Basic Research in Cardiology* vol. 104 131–139 (2009).
34. Perrelli, M.-G. Ischemia/reperfusion injury and cardioprotective mechanisms: Role of mitochondria and reactive oxygen species. *World J. Cardiol.* **3**, 186 (2011).
 35. Kischkel, F. C. *et al.* Cytotoxicity-dependent APO-1 (Fas/CD95)-associated proteins form a death-inducing signaling complex (DISC) with the receptor. *EMBO J.* **14**, 5579–5588 (1995).
 36. Van Cruchten, S. & Van den Broeck, W. Morphological and biochemical aspects of apoptosis, oncosis and necrosis. *Anat. Histol. Embryol.* **31**, 214–223 (2002).
 37. Vandenaabeele, P., Declercq, W., Van Herreweghe, F. & Berghe, T. Vanden. The role of the kinases RIP1 and RIP3 in TNF-induced necrosis. *Science Signaling* vol. 3 (2010).
 38. Zhang, D. W. *et al.* RIP3, an energy metabolism regulator that switches TNF-induced cell death from apoptosis to necrosis. *Science (80-.).* **325**, 332–336 (2009).
 39. Cho, Y. S. *et al.* Phosphorylation-Driven Assembly of the RIP1-RIP3 Complex Regulates Programmed Necrosis and Virus-Induced Inflammation. *Cell* **137**, 1112–1123 (2009).
 40. Feng, S. *et al.* Cleavage of RIP3 inactivates its caspase-independent apoptosis pathway by removal of kinase domain. *Cell. Signal.* **19**, 2056–2067 (2007).
 41. Lin, Y., Devin, A., Rodriguez, Y. & Liu, Z. G. Cleavage of the death domain kinase RIP by Caspase-8 prompts TNF-induced apoptosis. *Genes Dev.* **13**, 2514–

2526 (1999).

42. Murry, C. E., Jennings, R. B. & Reimer, K. A. Preconditioning with ischemia: A delay of lethal cell injury in ischemic myocardium. *Circulation* **74**, 1124–1136 (1986).
43. Marber, M. S., Latchman, D. S., Walker, J. M. & Yellon, D. M. Cardiac stress protein elevation 24 hours after brief ischemia or heat stress is associated with resistance to myocardial infarction. *Circulation* **88**, 1264–1272 (1993).
44. Kuzuya, T. *et al.* Delayed effects of sublethal ischemia on the acquisition of tolerance to ischemia. *Circ. Res.* **72**, 1293–1299 (1993).
45. Verdouw, P. D., Remme, W. J., de Jong, J. W. & Breeman, W. A. P. Myocardial substrate utilization and hemodynamics following repeated coronary flow reduction in pigs. *Basic Res. Cardiol.* **74**, 477–493 (1979).
46. Andrukhiv, A., Costa, A. D., West, I. C. & Garlid, K. D. Opening mitoKATP increases superoxide generation from complex I of the electron transport chain. *Am. J. Physiol. - Hear. Circ. Physiol.* **291**, (2006).
47. Yang, X., Cohen, M. V. & Downey, J. M. Mechanism of cardioprotection by early ischemic preconditioning. *Cardiovascular Drugs and Therapy* vol. 24 225–234 (2010).
48. Aruoma, O. I., Halliwell, B., Hoey, B. M. & Butler, J. The antioxidant action of N-acetylcysteine: Its reaction with hydrogen peroxide, hydroxyl radical, superoxide, and hypochlorous acid. *Free Radic. Biol. Med.* **6**, 593–597 (1989).

49. Sies, H. & Stahl, W. Vitamins E and C, β -carotene, and other carotenoids as antioxidants. in *American Journal of Clinical Nutrition* vol. 62 (Am J Clin Nutr, 1995).
50. Adlam, V. J. *et al.* Targeting an antioxidant to mitochondria decreases cardiac ischemia-reperfusion injury. *FASEB J.* **19**, 1088–1095 (2005).
51. Juriasingani, S., Akbari, M., Chan, J. Y., Whiteman, M. & Sener, A. H2S supplementation: A novel method for successful organ preservation at subnormothermic temperatures. *Nitric Oxide - Biol. Chem.* **81**, 57–66 (2018).
52. Zhu, C. *et al.* Supplementing preservation solution with mitochondria-targeted H2S donor AP39 protects cardiac grafts from prolonged cold ischemia–reperfusion injury in heart transplantation. *Am. J. Transplant.* **19**, 3139–3148 (2019).
53. Altesha, M. A., Ni, T., Khan, A., Liu, K. & Zheng, X. Circular RNA in cardiovascular disease. *Journal of Cellular Physiology* vol. 234 5588–5600 (2019).
54. Bayoumi, A. S., Aonuma, T., Teoh, J. P., Tang, Y. L. & Kim, I. M. Circular noncoding RNAs as potential therapies and circulating biomarkers for cardiovascular diseases review-article. *Acta Pharmacologica Sinica* vol. 39 1100–1109 (2018).
55. Sanger, H. L., Klotz, G., Riesner, D., Gross, H. J. & Kleinschmidt, A. K. Viroids are single stranded covalently closed circular RNA molecules existing as highly base paired rod like structures. *Proc. Natl. Acad. Sci. U. S. A.* **73**, 3852–3856 (1976).
56. Zheng, Q. *et al.* Circular RNA profiling reveals an abundant circHIPK3 that

- regulates cell growth by sponging multiple miRNAs. *Nat. Commun.* **7**, (2016).
57. Zeng, X., Lin, W., Guo, M. & Zou, Q. A comprehensive overview and evaluation of circular RNA detection tools. *PLoS Computational Biology* vol. 13 (2017).
 58. Ashwal-Fluss, R. *et al.* CircRNA Biogenesis competes with Pre-mRNA splicing. *Mol. Cell* **56**, 55–66 (2014).
 59. Vicens, Q. & Westhof, E. Biogenesis of circular RNAs. *Cell* vol. 159 13–14 (2014).
 60. Burset, M., Seledtsov, I. A. & Solovyev, V. V. Analysis of canonical and non-canonical splice sites in mammalian genomes. *Nucleic Acids Res.* **28**, 4364–4375 (2000).
 61. Jeck, W. R. & Sharpless, N. E. Detecting and characterizing circular RNAs. *Nature Biotechnology* vol. 32 453–461 (2014).
 62. Liang, D. & Wilusz, J. E. Short intronic repeat sequences facilitate circular RNA production. *Genes Dev.* **28**, 2233–2247 (2014).
 63. Conn, S. J. *et al.* The RNA binding protein quaking regulates formation of circRNAs. *Cell* **160**, 1125–1134 (2015).
 64. Galarneau, A. & Richard, S. Target RNA motif and target mRNAs of the Quaking STAR protein. *Nat. Struct. Mol. Biol.* **12**, 691–698 (2005).
 65. Hansen, T. B. *et al.* Natural RNA circles function as efficient microRNA sponges. *Nature* **495**, 384–388 (2013).
 66. Panda, A. C. Circular RNAs act as miRNA sponges. in *Advances in Experimental*

Medicine and Biology vol. 1087 67–79 (Springer New York LLC, 2018).

67. O'Brien, J., Hayder, H., Zayed, Y. & Peng, C. Overview of microRNA biogenesis, mechanisms of actions, and circulation. *Frontiers in Endocrinology* vol. 9 (2018).
68. Redfern, A. D. *et al.* RNA-induced silencing complex (RISC) Proteins PACT, TRBP, and Dicer are SRA binding nuclear receptor coregulators. *Proc. Natl. Acad. Sci. U. S. A.* **110**, 6536–6541 (2013).
69. Kai, D. *et al.* Circular RNA HIPK3 promotes gallbladder cancer cell growth by sponging microRNA-124. *Biochem. Biophys. Res. Commun.* **503**, 863–869 (2018).
70. Yu, H., Chen, Y. & Jiang, P. Circular RNA HIPK3 exerts oncogenic properties through suppression of miR-124 in lung cancer. *Biochem. Biophys. Res. Commun.* **506**, 455–462 (2018).
71. Zeng, K. *et al.* CircHIPK3 promotes colorectal cancer growth and metastasis by sponging miR-7 article. *Cell Death Dis.* **9**, (2018).
72. Shan, K. *et al.* Circular noncoding RNA HIPK3 mediates retinal vascular dysfunction in diabetes mellitus. *Circulation* **136**, 1629–1642 (2017).
73. Cao, Y., Yuan, G., Zhang, Y. & Lu, R. High glucose-induced circHIPK3 downregulation mediates endothelial cell injury. *Biochem. Biophys. Res. Commun.* **507**, 362–368 (2018).
74. Wang, L., Luo, T., Bao, Z., Li, Y. & Bu, W. J. Intrathecal circHIPK3 shRNA alleviates neuropathic pain in diabetic rats. *Biochem. Biophys. Res. Commun.* **505**, 644–650 (2018).

75. Cai, C. *et al.* CircHIPK3 overexpression accelerates the proliferation and invasion of prostate cancer cells through regulating miRNA-338-3p. *Oncotargets Ther.* **Volume 12**, 3363–3372 (2019).
76. Chen, D., Lu, X., Yang, F. & Xing, N. Circular RNA circHIPK3 promotes cell proliferation and invasion of prostate cancer by sponging miR-193a-3p and regulating MCL1 expression. *Cancer Manag. Res.* **11**, (2019).
77. Li, Y. *et al.* Circ HIPK 3 sponges miR-558 to suppress heparanase expression in bladder cancer cells. *EMBO Rep.* **18**, 1646–1659 (2017).
78. Okholm, T. L. H. *et al.* Circular RNA expression is abundant and correlated to aggressiveness in early-stage bladder cancer. *npj Genomic Med.* **2**, (2017).
79. Zhang, J. xiang *et al.* circHIPK3 regulates lung fibroblast-to-myofibroblast transition by functioning as a competing endogenous RNA. *Cell Death Dis.* **10**, (2019).
80. Ni, H. *et al.* Inhibition of circHIPK3 prevents angiotensin II-induced cardiac fibrosis by sponging miR-29b-3p. *Int. J. Cardiol.* **292**, 188–196 (2019).
81. Chen, B. *et al.* Circular RNA circHIPK3 Promotes the Proliferation and Differentiation of Chicken Myoblast Cells by Sponging miR-30a-3p. *Cells* **8**, 177 (2019).
82. Bai, M., Pan, C.-L., Jiang, G.-X., Zhang, Y.-M. & Zhang, Z. *CircHIPK3 aggravates myocardial ischemia-reperfusion injury by binding to miRNA-124-3p.*
83. Qiu, Z. *et al.* CircHIPK3 regulates the autophagy and apoptosis of

hypoxia/reoxygenation-stimulated cardiomyocytes via the miR-20b-5p/ATG7 axis. *Cell Death Discov.* **7**, 64 (2021).

84. Wang, Y. *et al.* Exosomal circHIPK3 Released from Hypoxia-Pretreated Cardiomyocytes Regulates Oxidative Damage in Cardiac Microvascular Endothelial Cells via the miR-29a/IGF-1 Pathway. *Oxid. Med. Cell. Longev.* **2019**, (2019).
85. Cheng, N., Jin, C., Jin, P., Zhu, D. & Hou, Z. High glucose protects cardiomyocytes against ischaemia/reperfusion injury by suppressing myocardiocyte apoptosis via circHIPK3/miR-29b/AKT3 signalling. *J. Cell. Mol. Med.* (2021) doi:10.1111/jcmm.16527.
86. Wang, Y. *et al.* Exosomal CircHIPK3 Released from Hypoxia-Induced Cardiomyocytes Regulates Cardiac Angiogenesis after Myocardial Infarction. *Oxid. Med. Cell. Longev.* **2020**, (2020).
87. Fleisher, T. A. Apoptosis. *Annals of Allergy, Asthma and Immunology* vol. 78 245–250 (1997).

EDUCATION

M.Sc Pathology and Laboratory Research

Fall 2019 to Present

The University of Western Ontario, London, Ontario

Bachelor of Science (*Specialization in Biochemistry*)

Fall 2015 to April 2019

Laurentian University, Sudbury, Ontario

RESEARCH EXPERIENCE

M.Sc Pathology and Laboratory Research

September 2019 - Present

The University of Western Ontario, London, Ontario

The role of circHIPK3 in Ischemic Reperfusion Injury

- Study the effects of circHIPK3 expression, knockdown and over-expression on cell viability during cardiac ischemia reperfusion injury
- Characterize circHIPK3 expression and biogenesis in cardiac ischemic reperfusion injury
- Investigate molecular mechanisms such as circRNA-miRNA and circRNA-Protein interactions using RNA immunoprecipitation (RIP)
- Translate circHIPK3 *in vitro* experiments to *in vivo* animal transplant model

Student Researcher

May 2017 – April 2019

Laurentian University, Sudbury, Ontario

Selective Method for Detection of H₂Se production from mammalian tissue

- Development of simple method to detect H₂Se production from mammalian tissue lysate
- Primary lead for all aspects of work including research direction

Investigation on the Interplay of H₂S/H₂Se in Cardiac Hypertrophy

- Study the interactions of H₂S/H₂Se systems in cystathionine gamma-lyase deficient mice and rat cardiomyocyte H9C2 cell line
- Build a reactive oxygen species (ROS) induced cardiac hypertrophy model using rat cardiomyocyte H9C2 cell line
- Use molecular techniques such as western blotting, PCR, fluorescent microscopy to study intracellular signal transduction

PUBLICATIONS

Department of Pathology and Laboratory Medicine, Western University, London, Ontario

- Bowen Wang, Qinfeng Zhou, Anthony Li, Shuailong Li, **Adam Greasley**, Anton Skaro, Douglas Quan, Weiping Min, Kexiang Liu, Xiufen Zheng., 2021, Preventing alloimmune rejection using circular RNA FSCN1-silenced dendritic cells in heart transplantation. *Journal of Heart and Lung Transplantation*.
- Yale Su, Cuilin Zhu, Bowen Wang, Hao Zheng, Vivian McAlister, James C Lacefield, Douglas Quan, Tina Mele, **Adam Greasley**, Kexiang Liu, Xiufen Zheng., 2020, Circular RNA Foxo3 in cardiac ischemia-reperfusion injury in heart transplantation: A new regulator and target. *American Journal of Heart Transplantation*.
- Duo Zhao, Hao Zheng, **Adam Greasley**, Fengjun Ling, Qinfeng Zhou, Bowen Wang, Tiffany Ni, Ishita Topiwala, Cuilin Zhu, Tina Mele, Kexiang Liu, Xiufen Zheng., 2020, The role of miR-711 in cardiac cells in response to oxidative stress and its biogenesis: a study on H9C2 cells. *Cellular & Molecular biology letters*. 9, 25:26

Cardiovascular and Metabolic Research Unit, Laurentian University, Sudbury, Ontario

- **Greasley A**, Belzile N, Yang G. H₂S protects against cardiac cell hypertrophy through regulation of selenoprotein. *Oxidative Medicine and Cellular Longevity*. 2019

Cardiovascular and Metabolic Research Unit, Laurentian University, Sudbury, Ontario

- Bourque C, Zhang Y, Fu M, Racine M, **Greasley A**, Pei Y, Wu L, Wang R, Yang G*. H₂S protects lipopolysaccharide-induced inflammation by blocking NFκB transactivation in endothelial cells. *Toxicol Appl Pharmacol*. 2017,338:20-29.

COMMUNICATION & INTERPERSONAL SKILLS

Hospital Volunteer

February 2014 to April 2017

Health Sciences North, Sudbury, Ontario

- Greet patients/visitors and direct/bring them to the location that they need to be for their appointment/to visit a patient or assist them with any possible questions
- Receive calls when volunteer assistance is required. Direct volunteers to the location where assistance is needed as well as document all volunteer activity for records
- Assist special needs children in recovery therapy pool

ORGANIZATION SKILLS

Laurentian Stem Cell Club Founder/President

January 2017 to Present

Sudbury, Ontario

- Organization of club, executive members, recruit new leaders and members
- Organize swabbing events including location, supplies, volunteer schedule
- Ensure all confidential swab kits were properly delivered to Canadian Blood Services

TEACHING EXPERIENCE

Teaching Assitant

January 2016 to April 2019

Laurentian University, Sudbury, Ontario

- Give directions to students performing in lab experiments in the fields of organic chemistry, biochemistry, and general chemistry
- Assist in marking of students reports

HONORS AND AWARDS

- Ontario Graduate Scholarship (OGS) **2020**
- 1st place SOUSCC speaker Biology and Medicine Division **2019**
- 2nd place Laurentian University Mini-symposium **2019**
- CGS Masters NSERC, Ottawa University (Declined Offer) **2019**
- Promising Biochemistry Student Award **2018/2019**
- NSERC USRA (2x) **2017/2018**
- Laurentian Academic Excellence Scholarship **2015/2016/2017/2018**